COMPARISON OF MECHANICAL PROPERTIES AND HEAT AFFECTED ZONE OF 304STAINLESS STEEL OF JOINTS BY TIG WELDING AND ELECTRIC ARC WELDING

A Thesis submitted
In partial fulfillment of the requirement
For the Degree

MASTER OF TECHNOLOGY(DUAL DEGREE)

In

MECHANICAL ENGINEERING

With specialization

In

"Production and Industrial Engineering"

By

AGAJUDDIN BEG
(Enrollment No. 1500101253)
Under the Supervision of
Mr. MAHMOOD ALAM

DEPARTMENT OF MECHANICAL ENGINEERING
INTEGRAL UNIVERSITY, LUCKNOW
JULY,2020

INTEGRAL UNIVERSITY

Lucknow

CERTIFICATE

Certified that **AGAJUDDIN BEG** (Enrollment No. 1500101253) has carried out the research work presented in this thesis entitled "**Comparison of Mechanical properties and heat affected zone of 304 stainless steel of joints by Tig and Electric arc welding"** for the award of **Master of Technology** from Integral University, Lucknow under our supervision. The thesis embodies result of original work, and studies are carried out by the student himself and the contents of the thesis do not form the basis for the award of any degree to the candidate or to anybody else from this or any other university/Institution.

Mr. Mahmood Alam
Department of Mechanical Engineering
Integral University, Lucknow I

Date: 09/09/2020 :

ABSTRACT

The present research work involves experimental investigation on optimization of seam and TIG welding parameters for SS304 Stainless Steel Sheets.

Resistance seam welding is a process that produces a weld at the surfaces of two similar metals. Like spot welding, seam welding and TIG welding relies on two electrodes, usually made from copper, to apply pressure and current. The electrodes are disc shaped and rotate as the material passes between them. This allows the electrodes to stay in constant contact with the material to make long continuous welds. The electrodes may also move or assist the movement of the material. Seam welding is a continuous joining process using electrode wheels on generally overlapping work pieces.

The materials used in these investigations were AISI 304, 304, 304 stainless steel with dimensions of 100mm X 50mm X 1.5 mm each were used as work piece materials. The joints were produced using seam and TIG welding process with welding parameters and levels using L27 array. Specimens for the mechanical testing were prepared as per ASTM standards. The hardness test for weld region was tested using Brinell hardness testing machine. The applied force was 1000 N and a 10 mm diameter ball indentor was used. The indentation after testing was measured using optical microscope. The standard formula was used to calculate the Brinell Hardness Number (BHN). The impact strength of the weld joints were determined using Izod specimen. The standard Izod test specimens were prepared for the test.

Taguchi approach was used for designing the experiments, L27 orthogonal array was applied which composed of three columns and 27 rows, which mean that 27 experiments were carried out. DOE was selected based on a three welding parameters with 3 levels each. The selected welding

parameters for this study are: welding pressure, welding speed and temperature. Taguchi method was applied to the experimental data using statistical software MINITAB 15.

In order to evaluate the influence of each selected factor on the responses: The signal-to-noise ratios S/N for each factor is to be calculated. The signals have indicated that the effect on the average responses and the noises were measured by the influence on the deviations from the average responses, which would indicate the sensitiveness of the experiment output to the noise factors.

The purpose of ANOVA is to find the significant factor statistically. It gives a clear picture as to how far the process parameter affects the response and the level of significance of the factor considered. The ANOVA table for mean and signal to noise ratio are calculated. The F test is being carried out to study the significance of the process parameter. The high F value indicates that the factor is highly significant in affecting the response of the process. In our investigation, welding speed is a highly significant factor and plays a major role in affecting the impact strength of the weld. Welding temperature is the most significant factor affecting the hardness of weld zone. Welding speed influences most on the impact strength of the weld joint among the selected parameters. Weld zone hardness is affected by the factor of welding temperature during seam welding and TIG welding of stainless steel sheets. Taguchi's design method can be effectively used for optimizing the welding parameters for both Seam welding and TIG welding techniques.

ACKNOWLEDGEMENT

I would like to express my deep sense of gratitude and respect to my supervisor **Mr. Mahmood Alam** for his invaluable guidance, motivation, constant inspiration and above all for his ever co-operating attitude that enabled me in bringing up this thesis in the present form. I consider myself extremely lucky to be able to work under the guidance of such a dynamic personality.

I am also thankful to **Dr. P.K. Bharti**, Head of Department, Mechanical Engineering, for his support and motivation.

I would also like to thank to "Central Institute of Plastic Engineering and Technology (CIPET), Nadarganj, Lucknow" who provided hardness testing and impact testing machine for successful completion of experimental work.

My very special thanks go to all my family members. Their love, affection and patience made this work possible and the blessings and encouragement of my beloved parents greatly helped me in carrying out this research work.

AGAJUDDIN BEG

Enl no- 1500101253

CHAPTER NO. **TITLE** **PAGE NO.**

CHAPTER NO. **TITLE** **PAGE NO.**

CHAPTER NO. **TITLE** **PAGE NO.**

LIST OF TABLES

LIST OF FIGURES

CHAPTER 1

INTRODUCTION

WELDING

Welding is a permanent joining process used to join different materials like metals, alloys or plastics, together at their contacting surfaces by application of heat and or pressure. During welding, the work-pieces to be joined are melted at the interface and after solidification a permanent joint can be achieved. Sometimes a filler material is added to form a weld pool of molten material which after solidification gives a strong bond between the materials. Weldability of a material depends on different factors like the metallurgical changes that occur during welding, changes in hardness in weld zone due to rapid solidification, extent of oxidation due to reaction of materials with atmospheric oxygen and tendency of crack formation in the joint position.

Welding is the least expensive process and widely used nowadays in fabrication. Welding can be done for different metals with the help of a number of processes in which heat is supplied either electrically or by means of a gas torch. Different welding processes are used in the manufacturing of automobile bodies, structural work, tanks, and general machine repair work. In the industries, welding is used in refineries and pipe line fabrication. It may be called a secondary manufacturing process.

Gas Welding

In gas welding process a focused high temperature flame produced by combustion of gas or gas mixture is used to melt the work pieces to be joined. An external filler material is used for proper welding. Most common type gas welding process is Oxy-acetylene gas welding where acetylene and oxygen reacts for producing some heat.

Arc Welding

In arc welding process an electric power supply is used to produce an arc between electrode and the work-piece material to join, so that work-piece metals melt at the interface and welding could be done. Power supply for arc welding process could be AC or DC type. The electrode used for arc welding could be consumable or non-consumable. For non-consumable electrode an external filler material could be used.

Types of Arc Welding

a. Consumable electrode welding
    i. Shielded metal arc welding (SMAW)
    ii. Gas metal arc welding (GMAW)
    iii. Flux-cored arc welding (FCAW)
    iv. Submerged arc welding (SAW)
b. Non-consumable electrode welding
    i. Gas tungsten arc welding (GTAW)
    ii. Plasma arc welding (PAW)

Shielded Metal Arc Welding (SMAW) or Manual Metal Arc Welding

This is the most common type of arc welding process, where a flux coated consumable electrode is used. As the electrode melts, the flux disintegrates and produces shielding gas that protect the weld area from atmospheric oxygen and other gases and produces slag which covers the molten filler metal as it transfer from the electrode to the weld pool. The slag floats to the surface of weld pool and protects the weld from atmosphere as it solidifies.

Gas Metal Arc Welding (GMAW) or Metal inert or active gas welding (MIG/MAG)

In this type of welding process a continuous and consumable wire electrode is used. A shielding gas generally argon or sometimes mixture of argon and carbon dioxide are blown through a welding gun to the weld zone.

Gas Tungsten Arc Welding (GTAW) or Tungsten Inert Gas (TIG)

GTAW or TIG welding process is an arc welding process uses a non consumable tungsten electrode to produce the weld. The filler metal is used in this process is tungsten. It has high melting point (330^0c). So the tungsten electrode will not be melted during welding. The weld area is protected from atmosphere with a shielding gas generally Argon or Helium or sometimes mixture of Argon and Helium. A filler metal may also feed manually for proper welding. GTAW most commonly called TIG welding process was developed during Second World War. With the development of TIG welding process, welding of difficult weld materials such as Aluminium

and Magnesium become possible. The use of TIG today has spread to a variety of metals like stainless steel, mild steel and high tensile steels, Al alloy, Titanium alloy. Like other welding system, TIG welding power sources have also improved from basic transformer types to the highly electronic controlled power source today.

Basic Mechanism of TIG Welding

TIG welding is an arc welding process that uses a non-consumable tungsten electrode to produce the weld. The weld area is protected from atmosphere by an inert shielding gas (argon or helium), and a filler metal is normally used. The power is supplied from the power source (rectifier), through a hand-piece or welding torch and is delivered to a tungsten electrode which is fitted in to the hand piece. An electric arc is then created between the tungsten electrode and the work piece using a constant-current welding power supply that produces energy and conducted across the arc through a column of highly ionized gas and metal vapours. The tungsten electrode and the welding zone are protected from the surrounding air by inert gas. The electric arc can produce temperatures of up to 20,000°c and this heat can be focused to melt and joint different part of material. The weld pool can be used to join the base metal with or without filler material. Schematic diagram of TIG welding and mechanism of TIG welding are shown in Figure 1.1 & respectively.

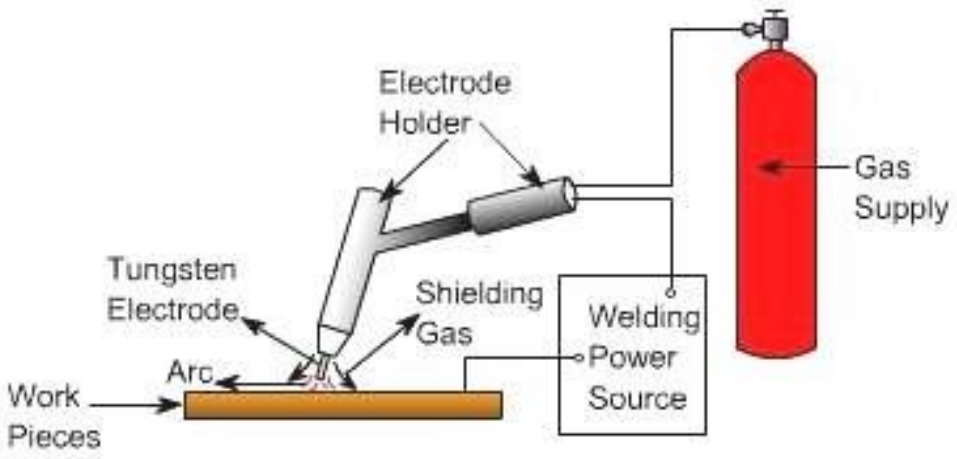

Source : http://nptel.ac.in/courses/112107144/welding/lecture10.htm

Figure 1.1 Schematic Diagram of TIG Welding System

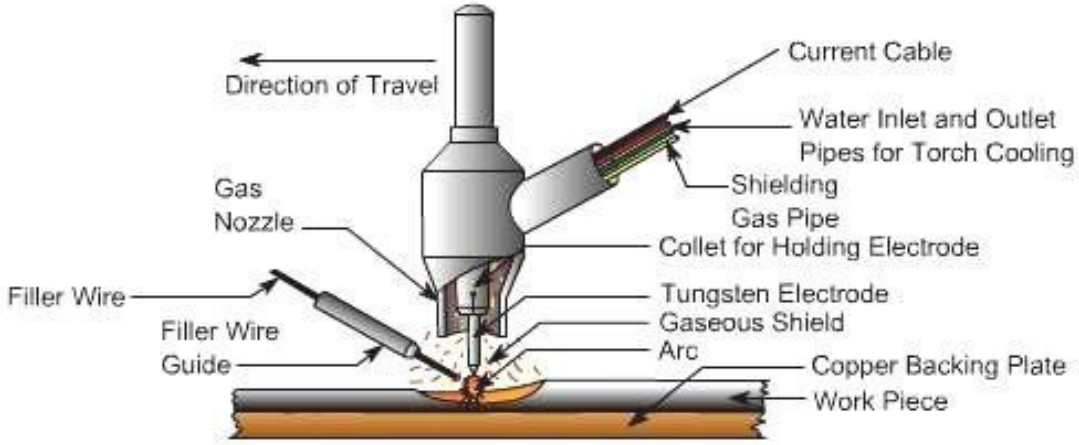

Source : http://nptel.ac.in/courses/112107144/welding/lecture10.htm

Figure 1.2 Principle of TIG Welding

Tungsten electrodes are commonly available from 0.5mm to 6.4mm diameter and 150-200mm length. The current carrying capacity of each size of electro depends on whether it is connected to negative or positive terminal of DC power source.

The power source required to maintain the TIG arc has a drooping or constant current characteristic which provides an essentially constant current output when the arc length is varied over several millimetres. Hence,

then the variations in the arc length which occur in manual welding have little effect on welding current. The capacity to limit the current to the set value is equally crucial when the electrode is short circuited to the work piece, otherwise excessively high current will flow, damaging the electrode. Open circuit voltage of power source ranges from 60 to 80V.

Types of welding current used in TIG welding

DCSP (Direct Current Straight Polarity)

In this type of TIG welding direct current is used. Tungsten electrode is connected to the negative terminal of power supply. This type of connection is the most common and widely used DC welding process. With the tungsten being connected to the negative terminal it will only receive 30% of the welding energy (heat). The resulting weld shows good penetration and an arrow profile.

DCRP (Direct Current Reverse Polarity)

In this type of TIG welding setting tungsten electrode is connected to the positive terminal of power supply. This type of connection is used very rarely because most heat is on the tungsten, thus the tungsten can easily over heat and burn away. DCRP produces a shallow, wide profile and is mainly used on very light material at low Amp.

AC (Alternating Current)

It is the preferred welding current for most white metals, e.g. aluminium and magnesium. The heat input to the tungsten is averaged out as the AC wave passes from one side of the wave to the other. On the half cycle, where the tungsten electrode is positive, electrons will flow from base material to the tungsten. This will result in the lifting of any oxide skin on the

base material. This side of the wave form is called the cleaning half. As the wave moves to the point where the tungsten electrode becomes negative the electrons will flow from the welding tungsten electrode to the base material. This side of the cycle is called the penetration half of the AC wave forms.

Alternating Current with Square Wave

With the advent of modern electricity AC welding machines can now be produced with a wave form called Square Wave. The square wave has better control and each side of the wave can give a more cleaning half of the welding cycle and more penetration.

Advantages of TIG welding

TIG welding process has specific advantages over other arc welding process. They are,

i. Narrow concentrated arc

ii. Able to weld ferrous and non-ferrous metals

iii. Does not use flux or leave any slag(shielding gas is used to protect the weld pool and tungsten electrode)

iv. No spatter and fumes during TIG welding

Applications of TIG Welding

The TIG welding process is best suited for metal plate of thickness around 5-6mm. Thicker material plate can also be welded by TIG using multi passes which results in high heat inputs, and leading to distortion and reduction in mechanical properties of the base metal. In TIG welding high quality welds can be achieved due to high degree of control in heat input and

filler additions separately. TIG welding can be performed in all positions and the process is useful for tube and pipe joint. The TIG welding is a highly controllable and clean process needs very little finishing or sometimes no finishing. This welding process can be used for both manual and automatic operations. The TIG welding process is extensively used in the so-called high-tech industry applications such as

i. Nuclear industry
ii. Aircraft
iii. Food processing industry
iv. Maintenance and repair work
v. Precision manufacturing industry
vi. Automobile industry

Process Parameters of TIG Welding

The parameters that affect the quality and outcome of the TIG welding process are given below.

Welding Current

Higher current in TIG welding can lead to splatter and work piece become damage. Again lower current setting in TIG welding lead to sticking of the filler wire. Sometimes larger heat affected area can be found for lower welding current, as high temperatures need to applied for longer periods of time to deposit the same amount of filling materials. Fixed current mode will vary the voltage in order to maintain a constant arc current.

Welding Voltage

Welding Voltage can be fixed or adjustable depending on the TIG welding equipment. A high initial voltage allows for easy arc initiation and a greater range of working tip distance. Too high voltage, can lead to large variable in welding quality.

Inert Gases

The choice of shielding gas depends on the working metals and effects on the welding cost, weld temperature, arc stability, weld speed, splatter, electrode life etc. It also affects the finished weld penetration depth and surface profile, porosity, corrosion resistance, strength, hardness and brittleness of the weld material. Argon or Helium may be used successfully for TIG welding applications. For welding of extremely thin material pure argon is used.

Argon generally provides an arc which operates more smoothly and quietly. Penetration of arc is less when Argon is used than the arc obtained by the use of Helium. For these reasons argon is preferred for most of the applications, except where higher heat and penetration is required for welding metals of high heat conductivity in larger thicknesses. Aluminium and copper are metals of high heat conductivity and are examples of the type of material for which helium is advantageous in welding relatively thick sections. Pure argon can be used for welding of structural steels, low alloyed steels, stainless steels, aluminium, copper, titanium and magnesium. Argon hydrogen mixture is used for welding of some grades of stainless steels and nickel alloys. Pure helium may be used for aluminium and copper. Helium argon mixtures may be used for low alloy steels, aluminium and copper.

Welding speed

Welding speed is an important parameter for TIG welding. If the welding speed is increased, power or heat input per unit length of weld decreases, therefore less weld rein for cement results and penetration of welding decreases. Welding speed or travel speed primarily control the bead size and penetration of weld. It is interdependent with current. Excessive high welding speed decreases wetting action, increases tendency of undercut, porosity and uneven bead shapes whiles lower welding speed reduces the tendency to porosity.

Resistance Welding

In resistance welding heat is generated due to passing of high amount current (1000–100,000A) through the resistance caused by the contact between two metal surfaces. Most common type resistance welding is Spot welding, where a pointed electrode is used. Continuous type spot resistance welding can be used for seam welding where a wheel-shaped electrode is used.

Resistance welding is a fusion welding process that requires the application of both heat and pressure to achieve a sound joint. The simplest form of the process is spot welding where the pressure is provided by clamping two or more overlapping sheets between two electrodes. A current is then passed between the electrodes, sufficient heat being generated at the interface by resistance to the flow of the current that melting occurs, a weld nugget is formed and an autogenous fusion weld is made between the plates. The heat generated depends upon the current, the time the current is passed and the resistance at the interface. The resistance is a function of the resistivity and surface condition of the parent material, the size, shape and material of the electrodes and the pressure applied by the electrodes.

There are a number of variants of the resistance welding process including spot, seam, projection and butt welding. It is an economical process ideally suited for producing large numbers of joints on a mass production basis. Spot welding in particular has been used extensively in the automotive industry, mostly for the joining of steel and in the aerospace industry for airframe components in aluminium alloys. Seam welding is used in the production of thin sheet, leak-tight containers such as fuel tanks.

There are a couple of characteristics of aluminium that make it more difficult to resistance weld than steel. The most significant is its high electrical conductivity, requiring high welding currents and large capacity equipment. Secondly, the electrodes are made from copper which alloys with aluminium, resulting in rapid wear and a short electrode life.

Types of Resistance Welding

i. Spot welding

ii. Seam welding

iii. Projection welding

iv. Resistance Butt welding

v. Flash Butt welding

Seam Welding

Resistance seam welding is a simple process that uses one or two wheels to apply pressure to the surface of two or more layers of conductive material. As the wheels roll, electric energy is applied using a capacitive discharge, high frequency, or line frequency weld controller in precise amounts to form a joint between the faying surfaces of the material. The resistance seam weld process is a fast, reliable and low cost way to join many

materials. Like most joining methods, it competes with other technologies like laser and TIG welding.

This method is a continuous spot welding process in which current is regulated by the timer of the machine. Seam welding consists of a continuous weld on two overlapping pieces of sheet metal that are held together under pressure between two circular electrodes. In high-speed seam welding using continuous current, the frequency of the current acts as an interrupter.

The heat at the electrode contact surfaces is kept to a minimum by the use of copper alloy electrodes and is dissipated by flooding the electrodes and weld area with water. Heat generated at the interface by contact resistance is increased by decreasing the electrode force. Another variable that influences the magnitude of the heat is the weld time, which in seam welding is controlled by the speed of rotation of the electrodes. The amount of heat generated is decreased with an increase in welding speed. The principle of seam welding is shown in Figure 1.3.

Principle of Seam Welding

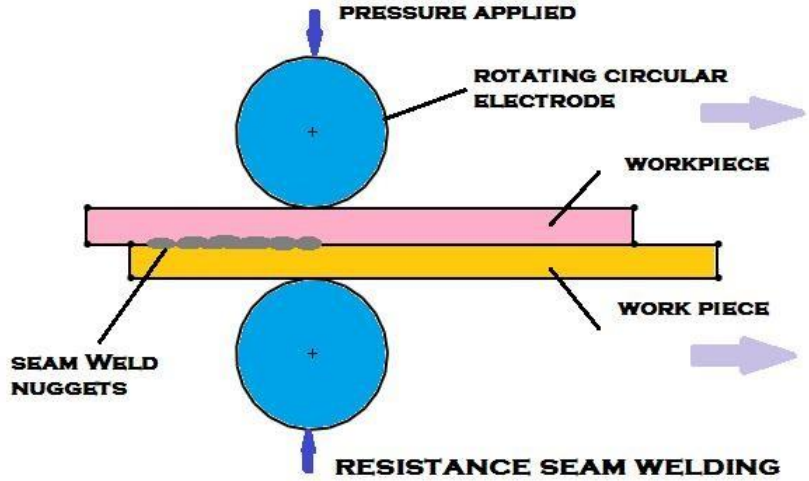

Source : http://marinenotes.blogspot.in/2013/01/resistance-seam-welding-and-types-of.html

Figure 1.3 Principle of seam welding

Resistance Seam Weld Types

Whether the seam weld is longitudinal, circular, or a unique planar contour, the weld nugget is formed in one of three ways

i. **Roll spot**

ii. **Overlapping spot**

iii. **Continuous seam**

The roll spot type occurs when there are distinct separations between the nuggets as the roller walks across the surface. If the weld schedule is fired at a constant repetition rate, the cross-section result looks like that shown in Figure 1.4.

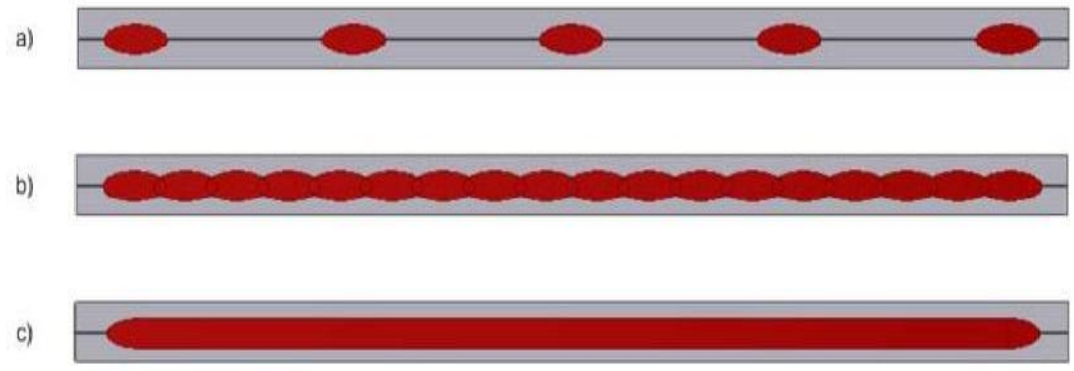

Source: Own Figure

Figure 1.4 Seam welding types a) Roll spot b) Overlap spot c) Continuous seam

Obviously, if one maintains the linear velocity, but increases the firing rate, the spots will get closer and closer together until they overlap. This is called overlap spot welding and creates a hermetic (i.e. leak tight) joint between the materials as depicted in Figure 1.4(a).

The overlap spot weld technique is very effective at joining thin materials (i.e. < 0.015” thick) without burn through. Continuous seam welding occurs when a constant stream of energy is applied to the rollers. This results in a joint like that in Figure 1.4(b).

Regardless of the type used, the electrodes are not opened between spots which results in a high speed joining process. Typical linear velocities for small scale resistance seam welding range from 0.2 to 1.0 in/sec and depend on the material type, part thickness, and weld schedule (one or two pulse) used. The roller force usually ranges from 5 to 75 lbs for thin materials, about 5 to 10 times that of a comparable pointed spot weld electrode using the same material thickness. The higher force is due to the additional surface area of the roller when compared to a straight electrode tip. The continuous seam welding is shown in Figure 1.4(c).

Operation of Seam Welding

i. The two work pieces to be joined are cleaned to remove dirt, grease and other oxides either chemically or mechanically to obtain a sound weld.

ii. The work pieces are overlapped and placed firmly between two wheel shaped copper alloy electrodes, which in turn are connected to a secondary circuit of a step-down transformer as shown in Figure 1.5.

iii. The electrode wheels are driven mechanically in opposite directions with the work pieces passing between them, while at the same time the pressure on the joint is maintained.

iv. Welding current is passed in series of pulses at proper intervals through the bearing of the roller electrodes wheels.

v. As the current passes through the electrodes, to the work piece, heat is generated in the air gap at the point of contact (spot) of the two work pieces. This is heat melts the work pieces locally at the contact point to form a spot weld.

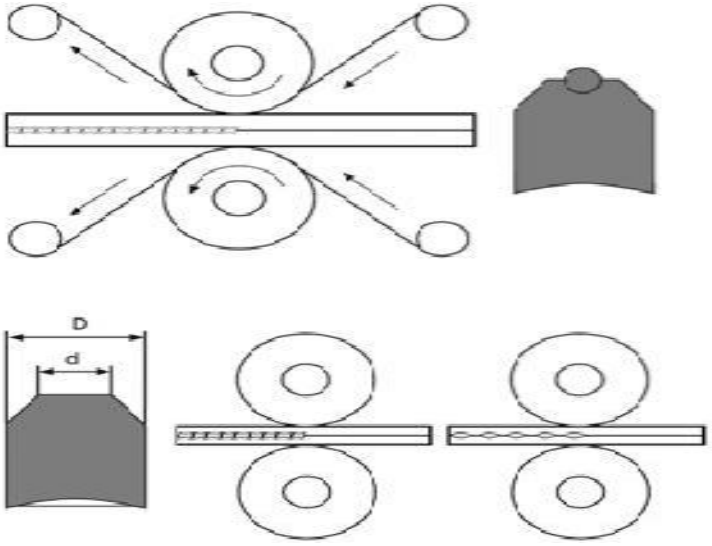

Source: Own Figure

Figure 1.5 Operation

vi. Under the pressure of continuously rotating electrodes and the current flowing through them, a series of overlapping spot welds are made progressively along the joint.

vii. The weld area is flooded with water to keep the electrode wheels cool during welding.

Advantages of Seam Welding

i. A continuous overlapping weld produced by the process makes it suitable for joining liquid or gas tight containers and vessels.

ii. Efficient energy use.

iii. Filler metals are not required. Hence, no associated fumes or gases. This results in clean welds.

iv. Seam welding can be used for manufacturing tight and pressure resistant welds in an efficient way.

v. Welding is fast and both coated and uncoated sheets can be welded.

vi. Seam welding can be used for joining sheets of different thickness, similar to other resistance welding methods.

vii. Seam welding is more difficult than other resistance welding methods when the total combined sheet thickness is over 3.5 mm.

viii. The cooling rate of the weld is slower in seam welding than when using other resistance welding methods.

ix. Therefore embrittlement, which occurs in the welding of high-strength steels, is less common in seam welding.

Disadvantages of Seam Welding

i. Requires complex control system to regulate the travel speed of electrodes as well as the sequence of current to provide satisfactory overlapping welds. The welding speed, spots per inch and timing schedule are all dependent on each other.

ii. Difficult to weld metals having thickness greater than 5mm.

Application of Seam Welding

i. Making rail car structural components

ii. Air frame sections

iii. Highway trailer components

iv. Automotive wheel covers

v. Wiper blade clips and holders

vi. Stove element clips

vii. Screen frames

viii. Toaster springs

ix. Curtain walls

High Energy Beam Welding

In this type of welding a focused energy beam with high intensity such as Laser beam or electron beam is used to melt the work pieces and join them together. These types of welding mainly used for precision welding or welding of advanced material or sometimes welding of dissimilar materials, which is not possible by conventional welding process.

Solid State Welding

Solid-state welding processes do not involve melting of the work piece materials to be joined. Common types of solid-state welding are

ultrasonic welding, explosion welding, electromagnetic pulse welding, friction welding, friction-stir-welding etc.

MATERIAL

Stainless Steel

In metallurgy, **stainless steel**, also known as **inox steel** or **inox** from French "inoxydable", is a steel alloy with a minimum of 10.5%chromium content by mass.

Stainless steel differs from carbon steel by the amount of chromium present. Unprotected carbon steel rusts readily when exposed to air and moisture. This iron oxide film (the rust) is active and accelerates corrosion by forming more iron oxide, and due to the greater volume of the iron oxide this tends to flake and fall away. Stainless steels contain sufficient chromium to form a passive film of chromium oxide, which prevents further surface corrosion by blocking oxygen diffusion to the steel surface and blocks corrosion from spreading into the metal's internal structure, and due to the similar size of the steel and oxide ions they bond very strongly and remain attached to the surface.

Stainless Steels are iron-based alloys that contain a minimum of about 12% Cr, the amount needed to prevent the formation of rust in unpolluted atmospheres (hence the designation stainless). Few stainless steels contain more than 30% Cr or less than 50% iron. They achieve their stainless characteristics through the formation of an invisible and adherent chromium rich oxide film. This oxide forms and heals itself in the presence of oxygen. Other elements added to improve particular characteristics include nickel, manganese, molybdenum, copper, titanium, silicon, niobium, aluminum, sulphur, and selenium. Carbon is normally present in amounts ranging from

less than 0.03% to over 1.0% in certain grades. Figure 1.6 provides a useful summary of some of the compositional and property linkages in the stainless steel family.

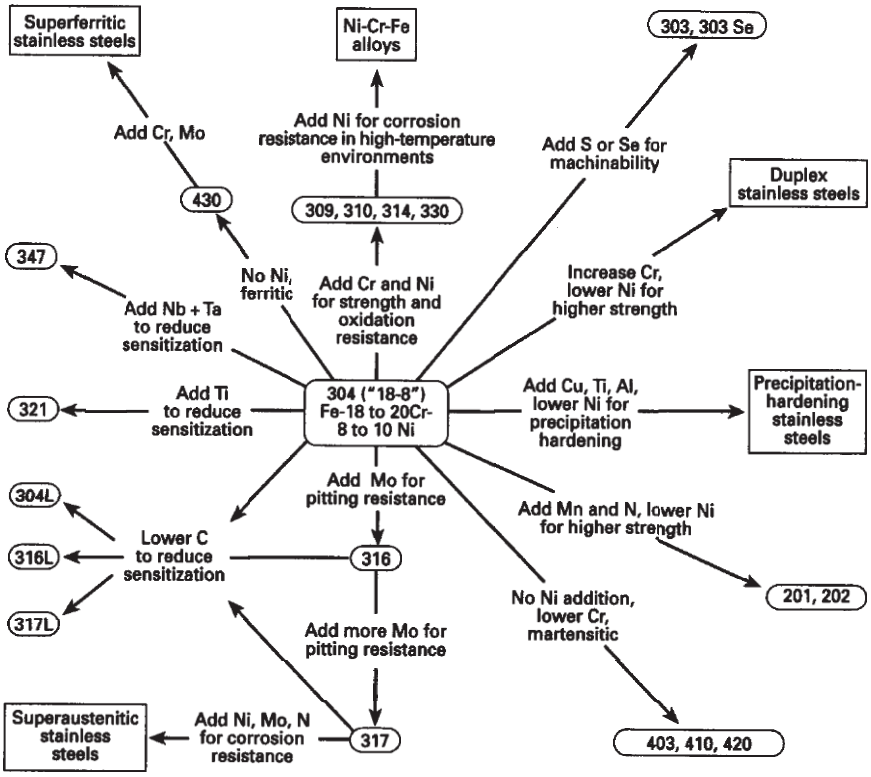

Source : https://www.google.co.in/search? espv=2&biw=1024&bih=677&tbm= isch&sa= 1&q=classifications +stainless+steel&oq=classifications+stainless+steel&gs_ l=img.3... 2058.5952.0.6124.0.0.0.0.0.0.0.0..0.0....0...1c.1.64.img..0.0.0.64qyHbBFqvg#imgrc=iAOck PlHb_6DKM%3A

Figure 1.6 Composition and property linkages in the stainless steel family of alloys

Production of Stainless Steels

With specific restrictions in certain types, the stainless steels can be shaped and fabricated in conventional ways. They are produced in cast, powder metallurgy (P/M), and wrought forms. Available wrought product forms include plate, sheet, strip, foil, bar, wire, semifinished products (blooms, billets, and slabs), pipe and tubing. Cold rolled flat products (sheet, strip, and plate) account for more than 60% of stainless steel product forms. Production of stainless steels is a two-stage process involving the melting of

scrap and ferroalloys in an Electric Arc Furnace (EAF) followed by refining by Argon Oxygen Decarburization (AOD) to adjust the carbon content and remove impurities. Alternative, melting, and refining steps include vacuum induction melting, vacuum arc re-melting, electro slag re-melting, and electron beam melting. Melting, and refining of stainless steels is, however, most frequently accomplished by the EAF/AOD processing route. In fact, about 90% of all stainless steel produced in the United States is processed by EAF melting followed by AOD.

During the final stages of producing basic mill forms sheet, strip, plate and bar and bringing these forms to specific size and tolerances, the materials are subjected to hot reduction with or without subsequent cold rolling operations, annealing, and cleaning. Further steps are required to produce other mill forms, such as wire and tube.

Applications of Stainless Steels

Stainless steels are used in a wide variety of applications. Most of the structural applications occur in the chemical and power engineering industries, which account for more than a third of the market for stainless steel products. These applications include an extremely diversified range of uses, including nuclear reactor vessels, heat exchangers, oil industry tubulars, components for chemical processing and pulp and paper industries, furnace parts, and boilers used in fossil fuel electric power plants.

Classification of Stainless Steels

Historically, stainless steels have been classified by microstructure and are described as austenitic, martensitic, ferritic, or duplex (austenitic plus ferritic). In addition, a fifth family, the precipitation-hardenable (PH) stainless steels, is based on the type of heat treatment used rather than the

microstructure. It should be noted that many of the wrought grades described below have cast counterparts.

Austenitic stainless steels constitute the largest stainless steel family in terms of alloys and usage. They include these grades:

i. Iron-chromium-nickel grades corresponding to both standard AISI 300-series alloys and modified versions of these alloys. Such alloys, which are based on type 304 (18-8) stainless steel generally contain 16 to 26% Cr, 10 to 22% Ni, and small amounts of other alloying elements such as molybdenum, titanium, niobium, and nitrogen.

ii. Iron-chromium-manganese-nickel grades corresponding to both standard AISI 200-series alloys and modified versions of these alloys. In these alloys, manganese (5 to 18%) replaces some of the nickel. Nitrogen alloying is also common with these alloys.

iii. Highly alloyed iron-nickel-chromium stainless steels for more severe corrosive environments. Nickel contents in these alloys can be as high as 35%. Molybdenum and copper additions are also common.

iv. Superaustenitic grades containing 6% Mo as well as liberal amounts of chromium, nickel, and nitrogen for improved corrosion resistance.

Ferritic Stainless Steels

Ferritic stainless steels are non hardenable iron-chromium alloys. They include the following:

i. Standard 400-series alloys as well as modified versions of these alloys containing 11 to 27% Cr, 0.08 to 20% C, and small amounts of ferrite stabilizers, such as aluminum, niobium, and titanium.

ii. More recently developed low interstitial content (low carbon/nitrogen) grades containing higher chromium (up to 30%), molybdenum (up to 4%), and nickel (up to 2%). Such grades, which exhibit excellent resistance to stress-corrosion cracking (SCC), are referred to as superferritics.

Martensitic Stainless Steels

Martensitic stainless steels are similar in composition to the ferritic group but contain higher carbon and lower chromium to permit hardening by heat treatment.

They include the following

i. Standard 400-series containing 11 to 18.0% Cr, up to 1.20% C, and small amounts of manganese and nickel.

ii. Nonstandard grades, including free-machining grades, heat-resistant grades, and grades for gears and bearings.

Duplex Stainless Steels

Duplex stainless steels are supplied with a microstructure of approximately equal amounts of austenite and ferrite. These alloys contain roughly 22 to 25% Cr, 5 to 7% Ni, up to 4% Mo, as well as additions of copper and nitrogen. Some of the more highly alloyed, corrosion resistant grades are referred to as super duplex stainless steels.

Duplex stainless steels are not covered by the standard AISI 200, 300, or 400 groups. While most have UNS numbers, some are also referred to by their chromium and nickel contents. For example, alloy 2205 contains 22% Cr and 5% Ni.

Precipitation Hardenable Stainless Steels

Precipitation hardenable stainless steels are chromium-nickel alloys containing alloy elements such as aluminum, copper, or titanium, which allow them to be hardened by a solution and aging heat treatment. They are further classified into subgroups as martensitic, semiaustenitic, and austenitic PH stainless steels. These steels are generally referred to by their tradename or UNS number.

Physical and Mechanical Properties of Stainless Steels

The physical and mechanical properties of stainless steels are quite different from those of commonly used nonferrous alloys such as aluminum and copper alloys. However, when comparing the various stainless families with carbon steels, many similarities in properties exist, although there are some key differences. Like carbon steels, the density of stainless steels is ~8.0 g/cm^3, which is approximately three times greater than that of aluminum alloys (2.7 g/cm^3). Like carbon steels, stainless steels have a high modulus of elasticity (200 MPa, or 30 ksi) that is nearly twice that of copper alloys (115 MPa, or 17 ksi) and nearly three times that of aluminum alloys (70 MPa, or 10 ksi). Differences among these materials are evident in thermal conductivity, thermal expansion, and electrical resistivity. The large variation in thermal conductivity among various types of materials; 6061 aluminum alloy (Al-lMg-0.6Si-0.3Cu-0.2Cr) has a very high thermal conductivity, followed by aluminum bronze (Cu-5Al), 1080 carbon steel, and then stainless

steels. For stainless steels, alloying additions, especially nickel, copper, and chromium, greatly decrease thermal conductivity.

Thermal expansion is greatest for type 6061 aluminum alloy, followed by aluminum bronze and austenitic stainless alloys, and then ferritic and martensitic alloys. For austenitic stainless alloys, additions of nickel and copper can decrease thermal expansion. Stainless steels have high electrical resistivity. Alloying additions tend to increase electric resistivity. Therefore, the ferritic and martensitic stainless steels have lower electrical resistivity than the austenitic, duplex, and PH alloys, but higher electrical resistivity than 1080 carbon steel. Electrical resistivity of stainless steels is ~7.5 times greater than that of aluminum bronze and nearly 20 times greater than that of type 6061 aluminum alloy.

Factors in Selection of Stainless Steels

The selection of stainless steels can be based on corrosion resistance, fabrication characteristics, availability, mechanical properties in specific temperature ranges, and product cost. However, corrosion resistance and mechanical properties are usually the most important factors in selecting a grade for a given application.

Characteristics to be considered in selecting the proper type of stainless steel for a specific application include these:

i. Corrosion resistance

ii. Resistance to oxidation and sulfidation

iii. Strength and ductility at ambient and service temperatures

iv. Suitability for intended fabrication techniques

v. Suitability for intended cleaning procedures

vi. Stability of properties in service

vii. Toughness

viii. Resistance to abrasion, erosion, galling, and seizing

ix. Surface finish and or reflectivity

x. Physical property characteristics, such as magnetic properties, thermal conductivity, and electrical resistivity.

xi. Total cost, including initial cost, installed cost, and the effective life expectancy of the finished product

xii. Product availability

Corrosion resistance is frequently the most important characteristic of a stainless steel but often is also the most difficult to assess for a specific application. General corrosion resistance to pure chemical solutions is comparatively easy to determine, but actual environments are usually much more complex.

General corrosion is often much less serious than localized forms such as SCC, crevice corrosion in tight spaces or under deposits, pitting attack, and inter-granular attack in sensitized material such as weld heat-affected zones. Such localized corrosion can cause unexpected and sometimes catastrophic failure while most of the structure remains unaffected, and, therefore, it must be considered carefully in the design and selection of the proper grade of stainless steel.

Corrosive attack can also be increased dramatically by seemingly minor impurities in the medium that may be difficult to anticipate but that can

have major effects, even when present in only parts-per-million concentrations. These effects can include heat transfer through the steel to or from the corrosive medium, contact with dissimilar metallic materials, stray electrical currents, and many other subtle factors. At elevated temperatures, attack can be accelerated significantly by seemingly minor changes in atmosphere that affect scaling, sulfidation, or carburization.

Despite these complications, a suitable steel can be selected for most applications on the basis of experience, perhaps with assistance from the steel producer. Laboratory corrosion data can be misleading in predicting service performance. Even actual service data have limitations, because similar corrosive media may differ substantially because of slight variations in some of the corrosion conditions listed previously. For difficult applications, extensive study of comparative data may be necessary, sometimes followed by pilot plant or in-service testing.

Other important factors that must be considered when selecting a stainless steel for a corrosion application include the following:

i. Chemical composition of the corrosive medium, including impurities

ii. Physical state of the medium: liquid, gaseous, solid or combinations

iii. Temperature

iv. Temperature variations

v. Aeration of the medium

vi. Oxygen content of the medium

vii. Bacteria content of the medium

viii. Ionization of the medium

ix. Repeated formation and collapse of bubbles in the medium

x. Relative motion of the medium with respect to the steel

xi. Chemical composition of the metal

Fabrication Characteristics

Stainless steels can be fabricated by methods similar to those used for carbon steels and other common metals. However, changes in fabrication methods may be necessary to the extent that stainless steels differ in yield strength and rate of work hardening. All have work hardening rates higher than common carbon steels, but the austenitics are characterized by large increases in strength and hardness with cold work. With the exception of the resulfurized free-machining grades, all stainless steels are suitable for crimping or flattening operations. The free-machining grades will withstand mild longitudinal deformation but may exhibit some tendency to splitting. In spite of their higher hardness, most martensitic and all of the ferritic types can be successfully fabricated.

Stainless Steel - Grade 304

Stainless Steel (304)

Stainless steel grade 304 is usually supplied in the form of strips and wires, with a tensile strength of up to 1800 Mpa, to produce tempers ranging from 1/16 Hard to Full Hard. By subjecting grade 304 to controlled analysis it is capable of retaining sufficient ductility even in ½ hard conditions. This form of grade 304 may be used in aircraft, rail car components and architectural structures.

Tempers of this grade, ranging from ¾ to full hard, may be used in applications requiring high wear resistance and spring features with simple form designs. Grade 304L, which is the low carbon form of grade 304, is the ideal choice for applications that require good ductility. Grade 304LN is another variant. This contains a higher percentage of nitrogen and exhibits a higher work harden rate compared to standard 304. The mechanical properties of SS304 steel is given in Table 1.1.

Types of Stainless Steel 304

i. Annealed

ii. ¼ hard

iii. ½ hard

iv. ¾ hard

v. Full hard

Mechanical Properties

Mechanical properties of 304 grade stainless steel

Table 1.1 The mechanical properties for stainless steel 304annealed, ½ hard and full hard is presented in Table

Grade	Tensile Strength (MPa) min	Yield Strength 0.2% Proof (MPa) min	Elongation (% in 50mm) min	Hardness	
				Rockwell B (HRB) max	Brinell (HB) max
304 annealed	515	205	40	32	297
304 1/2 hard	1034	758	18	32	297
304 full hard	1276	965	9	32	297

Source: http://www.aircraftmaterials.com/data/alstst/ams5517.html

Stainless Steel –Grade 304

Grade 304 is the standard molybdenum-bearing grade, second in importance to 304 amongst the austenitic stainless steels. The molybdenum gives 304 better overall corrosion resistant properties than Grade 304, particularly higher resistance to pitting and crevice corrosion in chloride environments. It has excellent forming and welding characteristics. It is readily brake or roll formed into a variety of parts for applications in the industrial, architectural, and transportation fields. Grade 304 also has outstanding welding characteristics. Post-weld annealing is not required when welding thin sections. Grade 304L, the low carbon version of 304 and is immune from sensitisation (grain boundary carbide precipitation). Thus it is extensively used in heavy gauge welded components (over about 6mm). Grade 304H, with its higher carbon content has application at elevated temperatures, as does stabilised grade 304Ti. The austenitic structure also gives these grades excellent toughness, even down to cryogenic temperatures. The mechanical properties of SS304 steel is given in Table 1.2.

Mechanical Properties

Mechanical properties of 304 grade stainless steel

Table 1.2 The mechanical properties for stainless steel 304, 304L, 304H is presented in Table.

Grade	Tensile Strength (MPa) min	Yield Strength 0.2% Proof (MPa) min	Elongation (% in 50mm) min	Hardness	
				Rockwell B (HRB) max	Brinell (HB) max
304	515	205	40	95	217
304L	485	170	40	95	217
304H	515	205	40	95	217

Source : http://www.atlassteels.com.au/documents/Atlas_Grade_datasheet_304 rev_Jan_2011.pdf

ORTHOGONAL ARRAY

An orthogonal array can assist, to determine how many trials are necessary, and the factor levels for each parameter in each trial. A parameter is an independent variable that may influence the final product, where as a level is a distinction within the parameter. Array selection is based on the number of parameters and the number of levels.

Consider a system which has 3 parameters and each of them as 3 values. To test all the possible combinations of these parameters (i.e, exhaustive testing) we will need a set of 3^3=27 test cases. But instead of testing the system for each combination of parameters, we can use an orthogonal array to select only a subset of this combinations. Using orthogonal array testing, we can maximize the test coverage while minimizing the number of test cases to consider. We here assume that the pair, that maximizes the interaction between the parameters, will have more defects and that the technique works.

Orthogonal Array Approach

The following terminologies have been used in this Approach,

1) Factor (f): Those parameters that the tester intentionally changes during testing to study its effect on the output.

2) Levels (p): The different values of factors used in testing.

During testing, we basically observe the average change in the response when a factor is changed from one level to another level.

As mentioned above, all these test cases can be executed in an ideal situation with infinite time and budget available. We are using orthogonal array approach to reduce the number of test cases.

The following steps are followed to construct the orthogonal array for testing a program with f factors, each factor having p levels:

1. Check if p is a prime number.
2. In case where each factor has different levels, Check whether the highest level is a prime number.
3. If the highest level not a prime, identify the next highest prime number.
4. Check if f <=p+1.If not, check if f is a prime number, else identify the next highest prime number.
5. There exists an OA (Orthogonal Array) with p2 rows and (p+1) columns.
6. When p=3, we have an OA with 9 rows and 4 columns.
7. We construct “p tuples” (e1, e2, ….ep) as follows:

   ei=(ei-1 + e1) mod p, for i= 3 to p

   e3 = (e2 + e1) mod 3 = (1,3,2)
8. Let us now construct the 9 rows and 4 columns.

Properties

Orthogonal array have number of unique properties

I. Equal proportions of experiments

II. Equal proportions of combinations of factor levels

III. Equal proportions of remaining factor levels

Signal to Noise Ratio

The quadratic loss function is ideally suited for evaluating the quality level of a product as it is shipped by a supplier to a customer. It typically has two components: one related to the deviation of the products function from the target, and other related to the sensitivity to the noise factor, signal to noise developed by Taguchi, is a predictor of quality loss after making certain adjustments to the product functions.

Taguchi's Technique

This Research work uses Taguchi method for optimization of welding parameters in welding of stainless steel, which is very attractive and effective method to deal with responses influenced by number of variables. In this method, main parameters are assumed to have influence on process results, which are located at different rows in a designed orthogonal array. With such an arrangement completely randomized experiments can be conducted. This method is useful for studying the interactions between the parameters, and also it is a powerful design of experiments tool, which provides a simple, efficient and systematic approach to determine optimal welding parameters. Compared to the conventional approach of experimentation, this method reduces drastically the number of experiments that are required to model the response functions. It is proposed for the purpose to improve the quality of products based on the concepts of statistics and engineering. The difference between the functional value and objective value is emphasized and identified as the loss function.

High signal-to-noise ratios are always preferred in Taguchi's experiments. For lower-the-better characteristic, this method translates into lower process average and improved consistency from one unit to the next or both. For analysis, there are 3 categories of performance characteristics, (i.e.) Smaller-the-better, Larger-the-better and Nominal-the-better.

Smaller-is-the better (Minimize)

$$S/N = -10\log\left\{\frac{1}{n}\sum_{i=1}^{n} y^2_i\right\}$$

Larger-is-the better (Maximize)

$$S/N = -10\log\left\{\frac{1}{n}\sum_{i=1}^{n}\frac{1}{y^2_i}\right\}$$

Nominal is the best

$$S/N = 10\log\left\{\frac{\bar{y}}{s^2_y}\right\}$$

In Taguchi method, for reducing the number of experiments and to determine the optimal welding parameters orthogonal array is introduced. Once the levels of each design parameters have been identified, analysis of the influence of welding parameters on hardness has been performed using response table for S/N ratios, which indicates the response at each level of control factors. Response tables are used to simplify the calculations needed to analyse the experimental data. The difference of factor on a response variable is the change in response when the factor goes from its level 1 to level 3. The higher the difference, the more influential the control factor is. The optimum level of welding parameters can be found from its

corresponding S/N ratios. The analysis of variance is performed finally to find the significant parameters.

Full factorial experimentation is time consuming and tedious when the number of factors are large. Use of taguchi's orthogonal array is advantageous, because it reduces the number of experiments. Taguchi experimental analysis was made using the popular software specifically used for design of experiment applications known as MINITAB 15. The predicted optimum is used to find the optimum value in mechanical testing.

ANOVA Method

The normal probability plot has the disadvantage of not providing a clear criterion for what values for estimated effects indicate significant factor or interaction effects, i.e., how far must a point be from the straight line pattern before it is judged to be an outlier? In addition, how do we measure amount of departure from the Straight-line pattern.

Analysis of variance (ANOVA) meets this need by how much an estimate must differ from zero in order to be judged "statistically significant". Analysis of variance (ANOVA) is a method of portioning variability into identifiable sources of variation and the associated degrees of freedom in an experiment.

In statistics, for analyzing the significant effect of the parameters on the quality characteristic, F test is used. It is assumed that there is no higher-level interaction. i.e., three factor and four factor interactions (also evident from response graph and normal probability plot) and hence average of squares of these estimated effects are used as the mean squared error.

This analysis was carried out for a level of significance of 5%, i.e., for a level of confidence of 95%.

QUALITY CHARACTERISTIC TESTING

1. Hardness test
2. Impact test

Brinell Hardness Test

One of the most popular hardness testing methods, Brinell Hardness Number is obtained using a perfectly spherical hardened steel ball of 10 mm pressed against the test surface using a static force of 3000 kg (=29.42 kilo Newton) for at least 10 seconds for steel and measuring the diameters of the indentation left on the surface by means of a graduated low power microscope. Figure 1.7 shows the hardness testing machine.

Source : https://www.google.co.in/search?espv=2&biw=1024&bih=677& tbm=isch &sa=1 &q=hardness+test&oq=hardness+test&gs_l=img.3... 49043.53666.0.53907 .0.0.0.0.0. 0.0. 0..0.0....0...1c.1.64.img..0.0.0.TeGsAS_ZXeI#imgdii=lAFTc7ku2WqmNM%3A%3BlAFTc 7ku2WqmNM%3A%3B25v2WRiNxPLwvM%3A&imgrc=lAFTc7ku2WqmNM%3A

Figure 1.7 Hardness Testing Machine

The equipment generally consists of a manually operated hydraulic press holding the test piece on a sturdy table and forcing a properly held ball indenter into the surface while avoiding impact.

Types of Indenters

The types of indenters are shown in Figure 1.8, 1.9 & 1.10.

1. Ball Indenter
2. Diamond Indenter

1. Ball Indenter

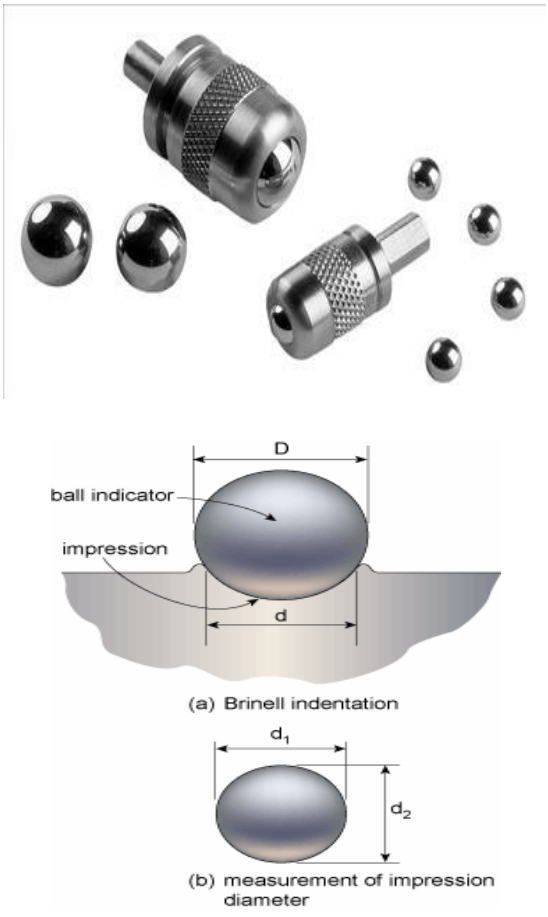

Source: https://www.google.co.in/search?espv=2&biw=1024&bih=677&tbm=isch&sa=1&q=hardness+test&oq=hardness+test&gs_l=img.3. 49043.53666.0.53907.0.0.0.0.0.0.0.0..0.0....0...1c.1.64.img..0.0.0.TeGsAS_ZXeI#imgrc=ZDaxs-HnIOoViM%3A

Figure 1.8 Ball indenter and impression

2. Diamond Indenter

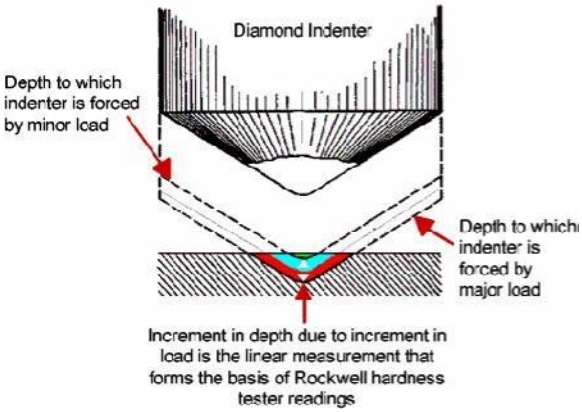

Source: https://www.google.co.in/search?espv=2&biw=1024&bih=677&tbm=isch&sa=1&q=indentor&oq=indentor&gs_l=img.3...57025.63221.0.63466.0.0.0.0.0.0.0.0..0.0....0...1c.1.64.img..0.0.0.ONW3Scr2fsQ#imgrc=O-XopAllPDnnHM%3A

Figure 1.9 Diamond indenter

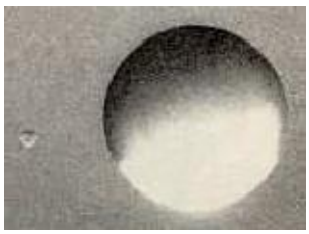

Source: https://www.google.co.in/search?q=brinell+hardness+impression&espv=2&source=lnms&tbm=isch&sa=X&ved=0ahUKEwitiZCg4vbLAhXFkI4KHfM6DRoQ_AUICCgC&biw=1024&bih=677#imgrc=J1ObgG5yiqxZDM%3A

Figure 1.10 Brinell Hardness Impression

Brinell Test Method

All Brinell tests use a carbide ball indenter. The test procedure is as follows:

i. The indenter is pressed into the sample by an accurately controlled test force.

ii. The force is maintained for a specific dwell time, normally 10 - 15 seconds.

iii. After the dwell time is complete, the indenter is removed leaving a round indent in the sample.

iv. The size of the indent is determined optically by measuring two diagonals of the round indent using either a portable microscope or one that is integrated with the load application device as shown in Figure 1.11.

v. The Brinell hardness number is a function of the test force divided by the curved surface area of the indent. The indentation is considered to be spherical with a radius equal to half the diameter of the ball. The average of the two diagonals is used in the following formula to calculate the Brinell hardness.

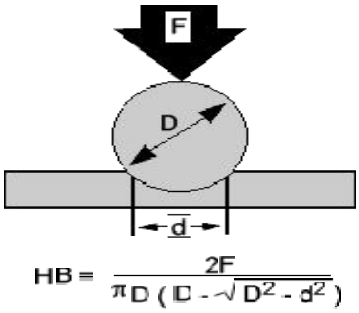

Source : http://www.instron.us/en-us/our-company/library/test-types/hardness-test/brinell-hardness-test

Figure 1.11 Indendation

The Brinell number, which normally ranges from HB 50 to HB 750 for metals, will increase as the sample gets harder. Tables are available to make the calculation simple.

Rockwell Hardness Machine

The Rockwell hardness test is an empirical indentation hardness test shown in Figure 1.12. Its worldwide adoption has likely resulted from the many advantages provided by the test method. The test is fast, inexpensive, and relatively non-destructive, leaving only a small indentation in the material. The simplicity in the operation of a Rockwell hardness machine has provided the added advantage that Rockwell hardness testing usually does not require a highly skilled operators.

Source : http://www.jmtt.com.cn/EnProductShow.asp?ID=74

Figure 1.12 Rockwell hardness machine

Impact Tests

Impact tests are designed to measure the resistance to failure of a material to a suddenly applied force. The test measures the impact energy, or the energy absorbed prior to fracture. Impact testing machine is shown in Figure 1.13.

The most common methods of measuring impact energy are the:

i. Charpy Test

ii. Izod Test

Charpy Impact Test

Measures the amount of energy absorbed during fracture of a specimen in a standard test. Testing includes sample preparation of 3

specimens per test. Usually applies to steels which exhibit temperature dependent behavior relating to toughness of the material at high strain. Toughness is typically related to direction of the rolling or grain flow of a forging. Materials are usually tougher along the direction of rolling and not as tough across the direction of rolling. This type of testing is typically required by welding codes in Pressure Vessels, valves and fittings used in the gas and oil industry, related piping, pipelines, and outdoor structures.

Izod Impact Test

Izod impact testing is a standard method of determining the impact resistance of materials. An arm held at a specific height is released. The arm hits the sample. The specimen either breaks or the weight rests on the specimen. From the energy absorbed by the sample, its impact energy is determined. A notched sample is generally used to determine impact energy and notch sensitivity.

Source : Photo image from our lab

Figure 1.13 Impact test arrangement

SCOPE OF THE PRESENT WORK

In this study, an attempt is made to conduct experiments on SS304 Stainless Steel sheets to study the weldability parameters during seam & TIG Welding.

The objectives of the research work are;

- To analyse the seam welding parameters of SS304 sheets using ANOVA and signal to noise to obtain maximum impact strength and hardness of the seam welded joints.
- To evaluate the weldability of stainless steel sheets (Grade 304) during TIG welding process using Taguchi Technique to accomplish maximum impact strength and hardness.
- To study the seam welding parameters of stainless steel (304) sheets using ANOVA and signal to noise to obtain maximum impact strength and hardness of the seam welded joints.

OVERVIEW OF THE THESIS

The thesis is organized as follows:

Chapter 1 – "Introduction", - presents briefly about scope and outline of welding, application of TIG and Seam Welding, Taguchi and its applications.

Chapter 2 – "Literature Review", - reports the literature review with the stainless steel, TIG welding, seam welding Taguchi, ANOVA, SN Ratio and weldability studies.

Chapter 3 – "Experimental Details", - deals with the selection of materials and their composition for the present study, TIG welding, Seam welding, Hardness Test, Impact Test and optimization using Taguchi Techniques.

Chapter 4 – "Results and discussion", - reports the analysis of the experimental results using various plots. The weldability of SS304, SS304 & SS304 are analysed and presented.

Chapter 5 – "Conclusion", presents the significant findings of the present investigation and their implications. Guidelines for future work are also included in this chapter.

At the end all the related references have been cited.

CHAPTER 2

LITERATURE SURVEY

INTRODUCTION

This chapter presents a comprehensive review of literature related to various types of welding process, welding materials, welding parameters, various behaviors of welding. A comprehensive overview of the earlier research work carried out in the area of welding process and optimization of various welding process is presented in detail in this chapter. The literature that laid a platform for the successful completion of the present investigation is mainly aimed to focus on the studies involving synthesis and mechanical behavior, metallurgical properties, welding temperature, Taguchi method, Design of Experiments, Welding parameters for stainless steel sheets.

Welding is the joining of materials in the welding zone with the use of heat and/or force, with or without filler metal. It can be facilitated with the help of, for example, shielding gases, welding powders, or pastes. However the energy required for welding is supplied by an esteemed source (M. Vural 2014)

WELDING MATERIALS

The study investigated the mechanical and metallurgical properties of friction-welded steel-aluminium and aluminium-copper bars, a friction welder having been designed and built for this purpose. The effects of the three main parameters: speed of rotation; friction load; and duration of

welding on the metallurgical and mechanical properties of the weld such as the yield, tensile and breaking strengths, are studied experimentally and statistically. The metallurgical properties of the weld are examined using electron and optical microscopy (Bekir Yilba et al. 1995).

Dissimilar metal joints of TiNi shape memory alloy wire and stainless steel wire were welded by laser welding method with and without Co filler metal. Comparative microstructure and properties of laser welded joints with and without Co filler metal have been investigated in detail. The effects of Co filler metal thickness on joint microstructure and properties were also discussed. The results indicated that the addition of Co filler metal had great effect to improve joint microstructure and properties. When 20 mm thick Co filler metal was used, the joint tensile strength and elongation reached the maximum values (347 MPa and 4.2%), and the corresponding joint fracture mode changed from pure brittle feature to mixture of cleavage and dimples due to decreasing brittle intermetallic compounds such as TiFe2, TiCr2, etc. But excessive Co addition resulted in decreasing the joint properties because of forming more Co–Ti intermetallic compounds (Hongmei Li et al. 2013).

Friction stir spot welding parameters affect the weld strength of thermoplastics, such as high density polyethylene (HDPE) sheets. The strength of a friction stir spot weld is usually determined by a lap-shear test. For maximizing the weld strength, the selection of welding parameters is very important. This paper presents an application of Taguchi method to friction stir spot welding strength of HDPE sheets. An orthogonal array, the signal to noise ratio (S/N), and the analysis of variance (ANOVA) are employed to investigate friction stir welding parameter effects on the weld strength. From the ANOVA and the S/N ratio response graphs, the significant parameters and the optimal combination level of welding parameters were obtained (Mustafa Kemal Bilici Ahmet IrfanYükler & Memduh Kurtulmus 2011).

The objectives of the study were to investigate the micro welding conditions related to diffusion mechanism and elemental migration metallurgical and microscopy investigation, and to establish the fundamental corrosion mechanism on the properties of small welding and brazing areas that consist different materials (Alaa Muhsin Saeed et al. 2010).

Thermoplastic polymer industry has expanded a new impact with the introduction of Eco-friendly thermoplastic matrix composites (TPCs), which finds applications in medical, aerospace, electronics and automotive areas. Joints of non-conductive thermoplastic composite materials are processed by Resistance Welding (RW) by incorporating a conductive corrosion resistive conductive material, as an interlayer. Glass fiber reinforced polypropylene thermoplastic composite sheets were used for this study. The experimental set-up for resistance welding was fabricated. Welding current, clamping pressure and welding duration (Time) are the control parameters. The joining trials on composites were carried out using Taguchi method to reduce time and cost effective experimental studies. The effect of parameters which govern the quality of resistance welding of thermoplastic composites is also emphasized in this work. The purpose of this study is to determine the optimum process parameters for Resistance welding. The joints obtained were analyzed microscopically; it revealed the good integration of thermoplastic composite with the interlayer material. The mechanical strength of the joints is tested through lap shear strength testing (Panneerselvama et al. 2012).

This work (Ivan J. de Santana Balsamo Paulo & Paulo J. Modenesi 2006) aims to develop and evaluate a piece of equipment to simulate high frequency induction welding of ferritic stainless steels using a conventional power supply for resistance spot welding. Modifications were performed in the power supply to allow but welding of thin sheet and variation of process parameters like sheet width, welding time and current. Tests were performed

to evaluate the use of this equipment. The results were evaluated by visual inspection, tensile testing and metallographic analysis. The analysis indicates that good-quality welds, which are similar to those obtained by high frequency welding, may be obtained

Magnesium alloy AZ31B sheets were welded using the technique of resistance spot welding with coverplates. The effects of welding parameters on the characteristics of the joint were investigated. The joint with larger nugget and higher tensile shear load was obtained under relatively low welding current condition. Enhancing electrode force and extending down-sloping time are effective for inhibiting pores formation and increasing the tensile shear strength of the joint under corresponding welding conditions. The results reveal that the technique is feasible to weld magnesium alloy (Hongxin Shi et al. 2010).

Two-wire tandem submerged arc welding process involves simultaneous depositions from two electrode wires with the leading wire usually connected to a DC power source and the trailing wire connected to a pulsed AC power source. The weld bead profile and mechanical properties in the tandem submerged welding are significantly affected by the leading and trailing wire current transients and the welding speed. The study presented a detailed experimental study on the influence of leading wire current, trailing wire current pulses, and welding speed on the weld bead dimensions and mechanical properties in single pass tandem submerged welding of a typical HSLA steel. It is realized that the weld bead penetration is primarily influenced by the leading wire current while the weld bead width and the reinforcement height are sensitive to the trailing wire current pulses. Greater magnitude of trailing wire current pulses and shorter negative pulse duration increase the weld pool volume leading to reduced cooling rate and poor mechanical properties

as the formation of the strengthening phases like acicular ferrite is inhibited. In contrast, increase in welding speed reduces the rate of heat input thereby enhancing the cooling rate and the weld bead mechanical properties. A set of empirical relations are developed to estimate the weld bead dimensions and mechanical properties as function of the welding conditions. The predictions from the empirical relations and the corresponding measured results are observed to be in fair agreement (Kirana et al. 2012).

Continuous drive friction welding studies on austenitic–ferritic stainless steel combination has been attempted in this investigation. Parameter optimization, microstructure–mechanical property correlation and fracture behaviour is a major contribution of the study. Sound welds are obtained at certain weld parameter combinations only. The mechanical properties of dissimilar metal welds are comparable to those of ferritic stainless steel welds. Evaluation of the joints for resistance to pitting corrosion revealed that the dissimilar welds exhibit lower resistance to pitting corrosion compared to the ferritic and austenitic stainless steel welds. Interface on the austenitic stainless steel side exhibited higher residual stress possibly due to its higher flow stress and higher coefficient of thermal expansion (Satyanarayana et al. 2005).

Friction welding method as a mass production process is finding increasing industrial acceptance, particularly for joining dissimilar materials. One of the areas using much more of the method is the tool industry. In this study (MuminSahin 2005), an experimental set-up was designed and produced to achieve the friction welding of components having equal diameter. The set-up was designed as continuous drive, and transition from friction to forging stage can be done automatically. In the experiments, high-speed steel (HSS—S 6-5-2) and medium-carbon steel (AISI 1040) were used. Post-weld annealing was applied to the joints at 650°C for 4 hours. First, the

optimum welding parameters for the joints were obtained. Later, the strengths of the joints were determined by tension, fatigue and notch-impact tests, and results were compared with the tensile strengths of materials. Then, hardness variations and microstructures in the post-weld of the joints were obtained and examined. Then, obtained results were compared with those of previous studies.

Stainless Steel 304

The aim of the study is to investigate experimentally the micro-structural properties and welding strengths of the joints using austenitic-stainless steel (AISI 304) parts. The experiments were carried out using a beforehand designed and constructed experimental friction welding set-up, constructed as continuous-drive. Firstly, pilot welding experiments under different friction time and friction pressure were carried out to obtain optimum parameters using statistical approach. Later, the strengths of the joints were determined by tension, fatigue and notch-impact tests, and results were compared with strengths of materials. Hardness variations and microstructures in the interfaces of the joints were also obtained and examined (MuminSahin 2007).

Austenitic-stainless steels are preferred over other stainless steels due to greater ease in welding. In the study, an experimental set-up was designed in order to achieve friction welding of plastically deformed austenitic-stainless steels. AISI 304 austenitic-stainless steels having equal and different diameters were welded under different process parameters. Strengths of the joints having equal diameter were determined by using a statistical approach as a result of tension tests. Hardness variations and microstructures using scanning electron microscope (SEM) analysis in the welding zone were obtained and examined. Subsequently, the effects on the welding zone of plastic deformation were analyzed. It has been established

that plastic deformation of AISI 304 austenitic-stainless steel has neither an effect on the process nor on the strength of the welding joint (MuminSahin 2009).

Friction welding (FW) is a process of solid state joining which is used extensively in recent years due to its advantages such as low heat input, production efficiency, ease of manufacture and environment friendliness. Friction welding can be used to join different types of ferrous metals and non-ferrous metals that cannot be welded by traditional fusion welding processes. The process parameters such as friction pressure, forging force, friction time and forging time play the major roles in determining the strength of the joints. In this investigation an attempt was made to develop an empirical relationship to predict the tensile strength of friction welded AA 6082 aluminium alloy and AISI 304 austenitic stainless steels joints, incorporating above said parameters. Response surface methodology (RSM) was applied to optimize the friction welding process parameters to attain the maximum tensile strength of the joint (Paventhan et al. 2011).

The purpose of the study is to propose a method to decide near optimal settings of the welding process parameters in friction welding of stainless steel (AISI 304) by using non conventional techniques and artificial neural network (ANN). The methods suggested in this study were used to determine the welding process parameters by which the desired tensile strength and minimized metal loss were obtained in friction welding. The study (Sathiya et al. 2009) describes how to obtain near optimal welding conditions over a wide search space by conducting relatively a smaller number of experiments. The optimized values obtained through these evolutionary computational techniques were compared with experimental results. The strength and microstructural aspects of the processed joints were also analyzed to validate the optimization.

Austenitic stainless steel cladding is generally used to attain better corrosion resistance properties to meet the requirements of petrochemical, marine, and nuclear applications. The quality of cladded components epends on the weld bead geometry and dilution, which in turn are controlled by the process parameters. The effect of cladding parameters such as welding current, welding speed, and nozzle-to-plate distance on the weld bead geometry was evaluated. The objective of controlling the weld bead geometry can easily be achieved by developing equations to predict these weld bead dimensions in terms of the process parameters. Mathematical equations were developed by using the data obtained by conducting three-factor five-level factorial experiments. The experiments were conducted for 317L flux cored stainless steel wire of size 1.2 mm diameter with IS:2062 structural steel as a base plate. Sensitivity analysis was performed to identify the process parameters exerting the most influence on the bead geometry and to know the parameters that must be most carefully controlled. Studies reveal that a change in process parameters affects the bead width, dilution, area of penetration, and coefficient of internal shape more strongly than it affects the penetration, reinforcement, and coefficient of external shape (Palani & Murugan 2006).

Linear friction welding is a solid state joining process established as a niche technology for the joining of aeroengine bladed disks. However, the process is not limited to this application, and therefore the feasibility of joining a common engineering austenitic steel, AISI 304L, has been explored. It was found that mechanically sound linear friction welds could be produced in 304L, with tensile properties in most welds exceeding those of the parent material. The mechanical properties of the welds were also found to be insensitive to relatively large changes in welding parameters. Texture was investigated in one weld using high energy synchrotron X-ray diffraction. Results showed a strong {111}(112) type texture at the centre of the weld,

which is a typical shear texture in face centre cubic materials. Variations in welding parameters were seen to have a significant impact on the microstructures of welds. This was particularly evident in the variation of the fraction of delta ferrite, in the thermo-mechanically affected zone of the welds, with different process parameters. Analysis of the variation in delta ferrite, with different welding parameters, has produced some interesting insights into heat generation and dissipation during the process. It is hoped that a greater understanding of the process could help to make the parameter optimisation process, when welding 304L as well as other materials, more efficient (ImranBhamji et al. 2010).

WELDING PROCESSES

Friction welding is a solid state joining process used extensively currently owing to its advantages such as slow heat input, high production efficiency, ease of manufacture, and environment friendliness. Materials difficult to be welded by fusion welding processes can be successfully welded by friction welding. An attempt was made to develop an empirical relationship to predict the tensile strength of friction welded AISI 1040 grade medium carbon steel and AISI 304 austenitic stainless steel, incorporating the process parameters such as friction pressure, forging pressure, friction time and forging time, which have great influence on strength of the joints. Response surface methodology was applied to optimize the friction welding process parameters to attain maximum tensile strength of the joint (Paventhan et al. 2012)

Friction stir spot welding (FSSW) is a new welding method which has recently been applied to polymeric materials. The feasibility of FSSW for two dissimilar polymers; polymethyl methacrylate (PMMA) and acrylonitrile butadiene styrene (ABS) was investigated. For this purpose, an improved tool equipped with an additional plate is used to make lap joint welded specimens.

The study also investigated the effect of FSSW parameters on mechanical properties of welded specimens (Saeid Hoseinpour Dashatan et al. 2013).

Robotic gas metal arc (GMA) welding is a manufacturing process which is used to produce high quality joints which can be utilized in automation systems to enhance productivity. Despite its widespread use in the various manufacturing industries, the full automation of the robotic GMA welding has not yet been achieved partly because mathematical models for the process parameters for a given welding tasks are not fully understood and quantified. The week proposed a neural network model to predict the weld bead width as a function of key process parameters in robotic GMA welding (Ill-Soo Kim et al. 2004)

A process of combined additive and subtractive techniques for the direct freeform fabrication of metallic prototypes and tools is being developed by the authors. This hybrid process, called '3D welding and milling', uses gas metal arc welding (GMAW) as an additive and conventional milling as a subtractive technique, thereby exploiting the advantages of both processes. The results of the optimization of the deposition process using a statistical approach as well as the result of plastic injection molding with the inserts fabricated by this hybrid process are described. The result proves the applicability of the 3D welding and milling process for direct fabrication of metallic prototypes and tools (Yong-AkSonga et al. 2005).

Results on friction welding of surface-hardened steels are analyzed based on experiments using induction-hardened steels as pivotal component, joined with quench-hardened steels and steels thermo chemically treated by carburization and nitriding, respectively. Higher axial pressure needs to be applied, inorder to fully expunge the hardened layers from the joining plane. A smooth surface for the burr, without cracks, can be obtained for adequate welding parameters and

the burr can be subsequently removed without major risks, immediately after the friction welding process ends. For joining an induction hardened C55 steel with a quenched hardened C55 steel, the maximal friction pressure has to be limited to about 200 N/mm^2, in order to avoid material separations in the centre of the joint. High axial pressures lead to good mechanical characteristic for friction welding an induction-hardened 34CrNiMo6 steel with a carburized 16MnCr5 steel. Friction welding of an induction-hardened C55 steel with a C45 nitrided steel showed that an increase of the friction upset distance to 6mm favours the complete expulsion of the nitride debris, with positive effects on the quality and mechanical properties of the joint (Ion Mitelea et al. 2012).

With the advance of the robotic welding process, procedure optimization that selects the welding procedure and predicts bead geometry that will be deposited has increased. A major concern involving procedure optimization should define a welding procedure that can be shown to be the best with respect to some standard, and chosen combination of process parameters, which give an acceptable balance between production rate and the scope of defects for a given situation. The article (Ill-SooKima et al. 2003) represents a new algorithm to establish a mathematical model for predicting top-bead width through a neural network and multiple regression methods, to understand relationships between process parameters and top-bead width, and to predict process parameters on top-bead width in robotic gas metal arc (GMA) welding process. Using a series of robotic GMA welding, additional multi-pass butt welds were carried out in order to verify the performance of the multiple regression and neural network models as well as to select the most suitable model. The results show that not only the proposed models can predict the top-bead width with reasonable accuracy and guarantee the uniform weld quality, but also a neural network model could be better than the empirical models.

Friction welding finds increasingly widespread industrial application as manufacturing method for joining parts. In the study, an experimental set up was designed and realised in order to achieve the friction welding of plastically deformed steel bars. The parts having same and different diameters deformed plastically, but same material was welded with different process parameters. The strengths of the joints were determined by tension tests. Hardness variations and microstructures in the welding zone were obtained and the effects of welding parameters on the welding zone were investigated (MuminSahin & ErolAkata 2003).

Compared to autonomous laser welding, the amount of parameters is higher for laser hybrid welding. Consequently, empirical optimisation of these parameters is a challenge. Handling and evaluation at a higher systematic level is desired in order to enhance the ability to build research on previous knowledge. Such new approach is studied on a case with 10 mm high strength steel sheets with fibre-laser hybrid weld. The week proposed to provide a method of documenting and handling data, transferable to other disciplines, to continuously build knowledge, to simplify repetition of experiments and to facilitate the start-up phase of new trials. Starting from 30 experimental results depending on 23 parameters, by the Matrix Flow Chart a guideline was developed that filters the information through combination, priorities and quality categorization. A chart resulted where five categories of poor quality are graphically related to a high quality category which can be achieved when following the guidelines for eight main arc- or laser-parameters. The chart is a guideline suitable for extension and for exploring the limits of its validity (Peter Norman et al. 2010).

A new welding method for fully automatic welding of pipelines was developed. The proposed welding procedure, called Friex, is a new variant of the well-known friction welding process. An intermediate ring is

rotated in between the pipes to be welded to generate the heat necessary to realize the weld. The working principles of the Friex welding process were briefly described (Koen Faes et al. 2009).

Electron beam welding is a highly efficient and precise welding method that is being increasingly used in industrial manufacturing and is of growing importance in industry. Compared to other welding processes it offers the advantage of very low heat input to the weld, resulting in low distortion in components. Modeling and simulation of the laser beam welding process has proven to be highly efficient for research, design development and production engineering. In comparison with experimental studies, a modeling study can give detailed information concerning the characteristics of weld pool and their relationship with the welding process parameters (welding speed, electron beam power, workpiece thickness, etc.) and can be used to reduce the costs of experiments (PiotrLacki & KonradAdamus 2011).

Vibration welding is a common method for creating complex hollow parts from simpler injection molded components. The studied the vibration welding of an industrial air intake manifold (AIM) made from nylon 66, nylon 6 and polypropylene all reinforced with 30%glass fibres. The meltdown-time profiles were measured and compared to those of simple lab-scale butt-weld assemblies. The experimental results indicated that the meltdown rate of the manifold was controlled by the slower rate of transverse welding. The burst strengths of these AIM at various welding conditions were also investigated. Results of finite element analysis indicated that the highest von Mises stresses and the maximum normal principle stresses at the weld region of the AIM were comparable to the weld strength of corresponding lab-scale coupons, confirming that the initial failure occurred in the weld region (Bates et al. 2004).

Magnesium alloys are being increasingly used in automotive and aerospace structures. Laser welding is an important joining method in such applications. There are several kinds of industrial lasers available at present, including the conventional CO_2 and Nd:YAG lasers as well as recently available high power diode lasers. A 1.5 kW diode laser and a 2 kW CO_2 lasers were used in the study for the welding of AZ31 alloys. It was found that different welding modes exist, i.e., keyhole welding with the CO_2 laser and conduction welding with both the CO2 and the diode lasers. The effect of beam spot size on the weld quality was analyzed. The laser processing parameters were optimized to obtain welds with minimum defects (Jinhong Zhu et al. 2005).

An experimental investigation of resistance welding of APC-2/AS4 PEEK/carbon fibre composite using a stainless steel mesh heating element was presented. A special specimen geometry, the skin/stringer configuration, was used to represent a typical reinforced aerospace structural joint. The specimens consisted of a flange, representing a stringer or frame, welded onto a skin laminate. The effects of the welding parameters such as the input power level and clamping distance on the weld quality and performance were investigated. The welding parameters were optimised using short beam shear tests, ultrasonic C-scan inspection and optical microscopy (Dube et al. 2007)

Simultaneous laser transmission welding process is systematically investigated via process modeling, using an FEM and RSM combined approach. The objective of the research was to study the effects of process parameters on the temperature field and weld bead dimensions. The thermal field is simulated by solving a three dimensional transient heat diffusion equation with temperature dependent material properties using the ANSYSs multi-physics. Response Surface Methodology is then applied for developing

mathematical models based on simulation results (Bappa Acherjee et al. 2012).

Fusion welding processes, such as resistance welding and laser welding, face difficulties in welding thin layers of dissimilar materials. Ultrasonic welding overcomes many of these difficulties by using high frequency vibration and pressure to input energy into the affected area to create a solid state weld. The paper presented a process robustness study of ultrasonic welding of thin metal sheets. Quality of the welded joints was evaluated based on mechanical tests and the quality criterion is then applied to evaluate the weldability. These results were used to determine both the optimal weld parameters and the robust operating range (Kim et al. 2011).

Friction-stir welding is a refreshing approach to the joining of metals. Although originally intended for aluminium alloys, the reach of FSW has now extended to a variety of materials including steels and polymers. This review deals with the fundamental understanding of the process and its metallurgical consequences. The focus is on heat generation, heat transfer and plastic flow during welding, elements of tool design, understanding defect formation and the structure and properties of the welded materials (Nandan et al. 2008).

New estimators are designed based on the modified force balance model to estimate the detaching droplet size and mean value of droplet detachment frequency in a gas metal arc welding process. The proper droplet size for the process to be in the projected spray transfer mode is determined based on the modified force balance model and the designed estimators. Finally, the droplet size and the melting rate are controlled using two proportional–integral (PI) controllers to achieve high weld quality by retaining the transfer mode and generating appropriate signals as inputs of the

weld geometry control loop (Mohammad Mousavi Anzehaee & Mohammad Haeri 2011).

Hybrid laser – metal active gas (MAG) arc welding is an emerging joining technology that is very promising for shipbuilding applications. This technique combines the synergistic qualities of the laser and MAG arc welding techniques, which permits a high energy density process with fit-up gap tolerance. As the heat input of hybrid laser – arc welding (HLAW) is greater than in laser welding, but much smaller than in MAG arc welding, a relatively narrow weld and restricted heat affected zone (HAZ) is obtained, which can minimize the residual stress and distortion. Furthermore, adding MAG arc can increase the penetration depth for a given laser power, which can translate to faster welding speeds or fewer number of passes necessary for one-sided welding of thick plates. New hybrid fiber laser – arc welding system was successfully applied to fully penetrate 9.3mm thick butt joints using a single-pass process through optimization of the groove shape, size and processing parameters (Cao et al. 2011).

Seam Welding

They (Goes et al. 2011) present a practical and robust methodology developed to evaluate the fatigue life of seam welded joints under combined cyclic loading. The finite element model was validated with the laboratory results. The analytical stress result presented upper value due to the approach used with considered the fillet weld supported in all work. The model presented a good representation of failure and load correlation. However, the thermal and metallurgical effects, such as distortions and residual stresses, were considered indirectly with regard to the corrections performed in the fatigue curves obtained from the investigated samples.

The (BingolM et al. 2007) focuses to investigate the effects of different extrusion parameters on micro structural properties of seam (longitudinal) welds in aluminum extrusion profiles. To realize the study, it is studied on a hollow extrusion profile type which has seam weld zones. The experimental profile was produced in different temperatures, billet temperatures and ram speeds by a real extrusion press which has a capacity of 1460 tones. These parameters are some of the most important parameters in an extrusion process. Some structural differences are occurred between different extrusion parameters. In addition, it was observed commonly the structure of the material had a change through re-crystallization with increasing temperatures. This situation decreases the significance of seam weld lines. Moreover, the grain size is getting smaller with increasing ram speed as it is shown in micro structural figures.

The (Massimo lanzoni et al. 2010) presented a Seam welding monitoring system able to detect faults in real time and with high sensitivity. The system is based on measurements and processing of electrical signals from sensors placed on the welding transformer and electrodes. Working prototypes of the system have been developed using commercial acquisition systems and high-quality conditioning electronics. Such prototypes have been implemented on commercial machines with excellent results. The system is able to perform accurate analysis in real time and allows remote assistance, management, and data collection. The system is based on widely available components and can be easily extended to include additional sensors.

Seam welds (Bingol & Keskin 2007) occur during the hollow profile extrusion; the billet’s material is divided into separate metal streams by the bridges of the die which support a mandrel, and then these metal streams are welded in welding chamber behind the bridges. When the desired conditions have not been provided, the required quality in seam welds may

not occur. One of the possible reasons for this situation is a poor metal feed. An insufficient pressure problem occurring in seam welds on an aluminum extrusion profile section was investigated. Findings: The poor metal feed occurring on specimen was shown by microstructural pictures. Microstructure of the main region has a homogenous appearance. In the microstructure, containing seam weld region, only a slight change was observed in seam weld region. However, there was no significant change in near of seam weld regions. This points out that there has been no metallurgical problem. Therefore, the problem is an insufficient pressure problem and this caused poor metal feeding. In the other hand, micro hardness tests are realized on seam weld region, main region and defective region's surround of specimen's section. Hardness values of seam weld region were lower than the main material's hardness values, but higher than the defective regions.

Experimental investigations were carried out using a pulsed neodymium:yttrium aluminum garnet laser weld to examine the influence of the pulse energy in the characteristics of the weld fillet. The pulse energy was varied from1.0 to 2.25 J at increments of 0.25 J with a 4ms pulse duration. The base material used for this study was AISI 304L stainless steel foil with 100µm thickness. The welds were analyzed by optical microscopy, tensile shear tests and micro hardness. The results indicate that pulse energy control is of considerable importance to thin foil weld quality because it can generate good mechanical properties and reduce discontinuities in weld joints. The ultimate tensile strength of the welded joints increased at first and then decreased as the pulse energy increased. The process appeared to be very sensitive to the gap between couples (Vicente AfonsoVentrellaa et al. 2010).

They (AmmarAzeez Mahdi et al. 2013) studied the effect of adding copper (C10200 AISI) foils on the seam welding joint of the austenitic stainless steel type (AISI 304).The austenitic stainless steel has low

weldability by resistance welding where the concentrated current causing a high thermal expansion.

TIG welding

The performance of silica coatings on TIG (or GTA) welding of AISI304L stainless steel was studied by investigating the effect of coating geometry and thickness on weld penetrations. Two coating designs were studied. One involves a 20 mm wide continuous coating across the weld zone and the second design formulates two parallel coatings 1–7 mm apart around the joint. The optimum thickness for continuous coatings is limited to about 50 μm whereas for 2 mm apart coatings, the optimum range extends from 70 to 200 μm. The presence of a narrow bare zone in the coating is suggested to be more practical for manual silica application. Tensile tests have been performed to identify the mechanical behavior in different characteristic zones of the welded specimens. The reduced tensile strength of the weld metal is attributed to the flux silica particles (Ruckert et al. 2007).

A neural network (Tarng et al. 1999) is used to construct the relationships between welding process parameters and weld pool geometry in tungsten inert gas (TIG) welding. An optimization algorithm called Simulated Annealing (SA) is then applied to the network for searching the process parameters with an optimal weld pool geometry. Finally, the quality of aluminum welds based on the weld pool geometry is classified and verified by a fuzzy clustering technique. Experimental results are presented to explain the proposed approach. The work pertains to the improvement of mechanical properties of AA 5456 Aluminum alloy welds through pulsed tungsten inert gas (TIG) welding process. Taguchi method was employed to optimize the pulsed TIG welding process parameters of AA 5456 Aluminum alloy welds for increasing the mechanical properties. Regression models were developed.

Analysis of variance was employed to check the adequacy of the developed models. The effect of planishing on mechanical properties was also studied and observed that there was improvement in mechanical properties. Microstructures of all the welds were studied and correlated with the mechanical properties (Kumar & Sundarrajan 2009).

Thermal stress analysis were performed in the tungsten inert gas (TIG) welding process of two different stainless steel specimens in order to compare their distortion mode and magnitude. The growing presence of non-conventional stainless steel species like duplex family generates uncertainty about how their material properties could be affected under the welding process. To develop suitable welding numerical models, the authors considered the welding process parameters, geometrical constraints, material non-linearities and all physical phenomena involved in welding, both thermal and structural. In this sense, four different premises are taken into account. Firstly, all finite elements corresponding to the deposition welding are deactivated and, next, they are reactivated according to the torch's movement to simulate mass addition from the filler metal into the weld pool. Secondly, the movement of the TIG torch was modelled in a discontinuous way by assuming a constant welding speed. Thirdly, the arc heat input was applied to the weld zone using volumetric heat flux distribution functions. Fourthly, the evolution of the structural response has been tackled through a stepwise non-linear coupled analysis. The numerical simulations are validated by means of full-scale experimental welding tests on stainless steel plates (del Coz Díaz et al. 2010).

A double-shielded TIG method was proposed to improve weld penetration and has been compared with the traditional TIG welding method under different welding parameters (i.e., speed, arc length and current). The strength of the Marangoni convection was calculated to

estimate the influence of the welding parameters on the variations in weld pool shapes. The results show that the changes in the welding parameters directly impact the oxygen concentration in the weld pool and the temperature distribution on the pool surface. The oxygen content and heat distribution on the weld pool surface are determinants of the pattern and strength of the Marangoni convection. For a negative temperature coefficient of surface tension (6o/6T<0), an outward Marangoni convection leads to a wide and shallow weld pool shape. The narrow and deep weld pool shape occurs when the Marangoni convection flows along an inward direction (6o/6T >0). The oxide layer that may appear with the relatively high oxygen content in the weld pool is harmful for the heat flow along the pool surface so as to reduce the welding efficiency especially in the double shielded TIG process (Dongjie Li et al. 2012).

The selection of process parameters (Juang & Tarng 2002) for obtaining an optimal weld pool geometry in the tungsten inert gas (TIG) welding of stainless steel was presented. Basically, the geometry of the weld pool has several quality characteristics, for example, the front height, front width, back height and back width of the weld pool. To consider these quality characteristics together in the selection of process parameters, the modified Taguchi method is adopted to analyze the effect of each welding process parameter on the weld pool geometry, and then to determine the process parameters with the optimal weld pool geometry. Experimental results are provided to illustrate the proposed approach.

TAGUCHI METHODS

In CO_2 continuous laser welding process was successfully applied and optimized for joining a dissimilar AISI 304stainless-steel and AISI 1009 low carbon steel plates. Laser power, welding speed and defocusing distance combinations were carefully selected with the objective of producing welded

joint with complete penetration, minimum fusion zone size and acceptable welding profile. Fusion zone area and shape of dissimilar austenitic stainless-steel with ferritic low carbon steel were evaluated as a function of the selected laser welding parameters. Taguchi approach was used as statistical design of experiment (DOE) technique for optimizing the selected welding parameters in terms of minimizing the fusion zone. Mathematical models were developed to describe the influence of the selected parameters on the fusion zone area and shape, to predict its value within the limits of the variables being studied (Anawa & Olabi 2008).

A design of experiment (DOE) technique, the Taguchi method, (Yousefieh1et al. 2012) was used to optimize the pulsed current gas tungsten arc welding (PCGTAW) parameters for the corrosion resistance of super duplex stainless steel (UNS S32760) welds. AL_9 orthogonal array (OA) of Taguchi design which involves nine experiments for four parameters (pulse current, background current, % on time, pulse frequency) with three levels was used. Corrosion resistance in 3.5%NaCl solution was evaluated by anodic polarization tests at room temperature. Analysis of variance (ANOVA) is performed on the measured data and S/N (signal to noise) ratios. The higher the better response category was selected to obtain optimum conditions. The optimum conditions providing the highest pitting potential were estimated. The optimum conditions were found as the second level of pulse current (120A), second level of background current (60A), third level of % on time (80) and third level of pulse frequency (5Hz). Under these conditions, pitting potential was predicted as $1.04V_{SCE}$ that was very close to the observed value of 1.06VSCE. As a result of Taguchi analysis in the study, the pulse current was the most influencing parameter on the corrosion resistance and the background current had the next most significant effect. The percentage contributions of pulse current, background current, % on time, and pulse frequency to the corrosion resistance were 66.28%, 25.97%, 2.71% and

5.04%, respectively. Consequently, the Taguchi method was found to be promising technique to obtain the optimum conditions for such studies. Moreover, the experimental results obtained confirm the adequacy and effectiveness of this approach.

A study carried out on 3.5 kW cooled slab laser welding of 904 L super austenitic stainless steel. The joints have butt welded with different shielding gases, namely argon, helium and nitrogen, at a constant flow rate. Super Austenitic Stainless Steel (SASS) normally contains high amount of Mo, Cr, Ni, N and Mn. The mechanical properties are controlled to obtain good welded joints. The quality of the joint is evaluated by studying the features of weld bead geometry, such as bead width (BW) and depth of penetration (DOP). The tensile strength and bead profiles (BW and DOP)of laser welded butt joints made of AISI 904 L SASS were investigated. The Taguchi approach was used as a statistical design of experiment (DOE) technique for optimizing the selected welding parameters. Grey relational analysis and the desirability approach were applied to optimize the input parameters by considering multiple output variables simultaneously. Confirmation experiments was conducted for both of the analyses to validate the optimized parameters (Sathiya et al. 2011).

Taguchi approach was applied to determine the most influential control factors which will yield better tensile strength of the joints of friction stir welded RDE-40 aluminium alloy. In order to evaluate the effect of process parameters such as tool rotational speed, traverse speed and axial force on tensile strength of friction stir welded RDE-40 aluminium alloy, Taguchi parametric design and optimization approach was used. Through the Taguchi parametric design approach, the optimum levels of process parameters were determined. The results indicate that the rotational speed, welding speed and axial force are the significant parameters in deciding the

tensile strength of the joint. The predicted optimal value of tensile strength of friction stir welded RDE-40 aluminium alloy is 303 MPa. The results were confirmed by further experiments (Lakshminarayanan & Balasubramanian 2008).

Laser welding with (Yang dongxia et al. 2012), filer wire was successfully applied to joining a new-type Al–Mg alloy. Welding parameters of laser power, welding speed and wire feed rate were carefully selected with the objective of producing a weld joint with the minimum weld bead width and the fusion zone area. Taguchi approach was used as a statistical design of experimental technique for optimizing the selected welding parameters. From the experimental results, it was found that the effect of welding parameters on the welding quality decreased in the order of welding speed, wire feed rate, and laser power. The optimal combination of welding parameters is the laser power of 2.4 kW, welding speed of 3 m/min and the wire feed rate of 2 m/min. Verification experiments was also conducted to validate the optimized parameters.

The use of grey-based (Tarng et al. 2002), Taguchi methods for the optimization of the submerged arc welding (SAW) process parameters in hard facing with considerations of multiple weld qualities was reported by Tarng et. al. In this new approach, the grey relational analysis was adopted to solve the SAW process with multiple weld qualities. A grey relational grade obtained from the grey relational analysis was used as the performance characteristic in the Taguchi method. Then, optimal process parameters were determined by using the parameter design proposed by the Taguchi method. Experimental results have shown that optimal SAW process parameters in hard facing can be determined effectively so as to improve multiple weld qualities through this new approach.

The effect of each welding parameter on the weld bead geometry, and then sets out to determine the optimal process parameters using the Taguchi method to determine the parameters was reported by (Her-Yueh Huang 2010). Three kinds of oxides, Fe2O3, SiO2, and MgCO3, were used to investigate the effect of activating flux aided gas metal arc welding (GMAW) on weld bead geometry, angular distortion and mechanical properties in AISI 1020 carbon steel.

The use of an Nd:YAG laser for thin plate magnesium alloy butt welding was optimized using the Taguchi analytical methodology. The welding parameters governing the laser beam in thin plate butt welding were evaluated by measuring the ultimate tension stress. The effectiveness of the Taguchi method lies in clarifying the factor that dominates complex interactions in laser welding. The factors are the shielding gas, laser energy, convey speed of workpiece, point at which the laser is focused, pulse frequency, and pulse shape. Furthermore, 18 combinations of these six essential welding parameters were set and Taguchi's method followed exactly.

The optimal result was confirmed with a superior ultimate tension stress of 169 MPa, 2.5 times larger to that from original set for laser welding (Lung Kwang Pana et al. 2004).

Experimental and numerical results of friction stir spot welding of high density polypropylene were reported. The determination of the welding parameters plays an important role for the weld strength. The experimental tests, conducted according to combinations of process factors such as tool rotation speed, plunge depth and dwell time at the beginning of welding, were carried out according to Taguchi orthogonal table L9 in randomized way. The Taguchi approach was used as a statistical design of experiment technique to set the optimal welding parameters. The results show coherence between the

numerical predictions and experimental observations in different cases of weld strength (Mustafa Kemal Bilici 2012).

WELDING PARAMETER OPTIMIZATION

When an aluminum pipe is welded circumferentially under constant welding conditions, the width and depth of the weld bead increase gradually along the welding direction. Therefore, the welding parameters should be optimized continuously to obtain a uniform weld bead along the entire circumference of the pipe. A state equation governing the heat flow in circumferential pipe welding is analyzed using a semi-analytical finite-element method, and optimal welding parameters were obtained using a state-space method. As the welding parameters to be optimized, the welding velocity, the effective radius of heat source and the heat input are considered. The sequences of welding parameters was optimized and compared with experimental results to verify the accuracy of the proposed model. The weld-pool geometry measured along the entire weld was found to be almost the same as the calculated results, a uniform weld bead around the pipe circumference being obtained. Three process parameter were optimized at the beginning of process optimization to obtain their proper initial values, and then only the heat input, which can be controlled easily with a conventional welding machine, was considered as the optimization parameter, in order to reduce the amount of calculation involved (Na & Lee 1996).

A statistical analysis of the electron beam welding of stainless steel samples was done using multiresponse statistical techniques. A model is created which includes the values of the distance between the electron gun and both the focusing plane of the beam and the sample surface as parameters. The response at work surfaces for the welding depth and width for variable beampower, welding speed, and the above two distances, determining the position of the beam focus towards the sample surface can be found. These

predicted results coincide with the existing experimental experience in this technique. A simultaneous modeling of the behavior of the weld parameters depth and width has been made in correlation with the parameters used: electron beam power, welding velocity, distance from the main surface of the magnetic lens of the gun to the focus of the electron beam and the distance between the magnetic lens and the surface of the sample within some region of interest. This sequence of techniques can be applied to different welding machines and the obtained models and results will differ for every single case. The influence of other welding parameters can also be explored (ElenaKoleva 2001).

Thermal efficiency is considered in connection with welding regimes and seam parameters by applying a statistical approach. This approach allows one to establish empirically (by fitting a mathematical model) the type of relationship that is present between performance characteristics and its influencing factors. Optimal regimes are found through thermal efficiency optimization. The study leads to new proposals for the position of the focus with respect to the surface of the welded material, under conditions of maximum thermal efficiency or maximum welding depth. The values of the ratio of power to weld depth and weld width times velocity of weld front are confirmed to be the main characteristic parameters of electron beam welding, considered as a self-organising process (Koleva 2005).

It concerns mathematical and numerical modeling of thermal phenomena accompanying single laser and laser-arc hybrid butt welding of steel sheets. Coupled heat transfer and fluid flow in the fusion zone were described respectively by transient heat transfer equation and Navier–Stokes equation. Laser beam and electric arc heat sources were modeled using different heat source power distributions. Latent heat associated with the material’s state changes, buoyancy forces and liquid material flow through

aporous medium were taken in to account in considerations. Differential governing equations were numerically solved using projection method combined with finite volume method. Elaborated solution algorithm was implemented into computer solver used for simulation of heat transfer and fluid flow during welding. The geometry of the weld and heat affected zone as well as cooling rates were estimated on the basis of numerically obtained temperature field (Piekarska & Kubiak 2012).

Resistance spot welding (RSW) was employed to pre-join refractory alloy 50Mo–50Re (wt%) sheet with a 0.127 mm gage. Five important welding parameters (hold time, electrode, ramp time, weld current and electrode force) were adjusted in an attempt to optimize the welding quality. It was found that increasing the hold time from 50 minutes to 999 minutes improved the weld strength. Use of rod-shaped electrodes produced symmetric nugget and enhanced the weld strength. Use of a ramp time of 8 minutes minimized electrode sticking and molten metal expulsion. The weld strength continuously increased with increasing the weld current up to 1100 A, but the probabilities of occurrence of electrode sticking and molten metal expulsion were also increased. Electrode force was increased from 4.44 N to 17.8 N, in order to reduce the inconsistency of the welding quality. Welding defects including porosities, columnar grains and composition segregation were also studied (JianhuiXu et al. 2007).

Resistance seam welding is a process that produces a weld at the surfaces of two similar metals. Like spot welding, seam welding relies on two electrodes, usually made from copper, to apply pressure and current. The electrodes are disc shaped and rotate as the material passes between them. This allows the electrodes to stay in constant contact with the material to make long continuous welds. The electrodes may also move or assist the movement of the material. Seam welding is a continuous joining process

using electrode wheels on generally overlapping workpieces. The Taguchi method is one of the techniques that could be applied to optimize the input welding parameters. Optimization of process parameters is the key step in the Taguchi method in achieving high quality, without increasing the cost. The optimal process parameters obtained from the Taguchi method are insensitive to the variation of environmental conditions and other noise factors (Sathiya et al. 2011).

An empirical relationship is developed to predict tensile strength of the laser beam welded AZ31B magnesium alloy by incorporating process parameters such as laser power, welding speed and focal position. The experiments were conducted based on a three factor, three level, central composite face centered design matrix with full replications technique. The empirical relationship can be used to predict the tensile strength of laser beam welded AZ31B magnesium alloy joints at 95% confidenc level. The results indicate that the welding speed has the greatest influence on tensile strength followed by laser power and focal position (Padmanaban & Balasubramanian 2010).

Generally, the quality of a weld joint is directly influenced by the welding input parameter settings. Selection of proper process parameters is important to obtain the desired weld bead profile and quality. Numerical and graphical optimization techniques of the CO_2 laser beam welding of dual phase (DP600)/transformation induced plasticity (TRIP700) steel sheets were carried out using Response Surface Methodology (RSM) based on Box–Behnken design. The procedure was established to improve the weld quality, increase the productivity and minimize the total operation cost by considering the welding parameters range of laser power (2–2.2 kW), welding speed (40–50 mm/s) and focus position (1 to 0 mm). It was found that, RSM can be considered as a powerful tool in experimental welding optimization, even

when the experimenter does not have a model for the process. Strong, efficient and low cost weld joints could be achieved using the optimum welding conditions (Reisgen et al. 2012).

Generally, the quality of a weld joint is directly influenced by the welding input parameter settings. Selection of proper process parameters is important to obtain the desired weld bead profile and quality. Reisgen et al. carried out work on numerical and graphical optimization techniques of the CO2 laser beam welding of dual phase transformation induced plasticity steel sheets using response surface methodology (RSM) based on Box–Behnken design. They have established procedure to improve the weld quality, increase the productivity and minimize the total operation cost by considering the welding parameters range of laser power, welding speed and focus position. It was found that, RSM can be considered as a powerful tool in experimental welding optimization, even when the researcher does not have a model for the process (Reisgen et al. 2012).

Laser butt-welding of medium carbon steel was investigated using CW1.5 kWCO_2 laser. The effect of laser power (1.2–1.43 kW), welding speed (30–70 cm/min) and focal point position (−2.5 to 0mm) on the heat input and the weld-bead geometry (i.e. penetration (P), welded zone width (W) and heat affected zone width (W_{HAZ})) was investigated using Response Surface Methodology (RSM). The experimental plan was based on Box–Behnken design. Linear and quadratic polynomial equations for predicting the heat input and the weld-bead geometry were developed. The results indicate that the proposed models predict the responses adequately within the limits of welding parameters being used. It is suggested that regression equations can be used to find optimum welding conditions for the desired criteria (Benyounis et al. 2005).

Laser welding input parameters play a very significant role in determining the quality of a weld joint. The joint quality can be defined in terms of properties such as weld bead geometry, mechanical properties and distortion. Therefore, mechanical properties should be controlled to obtain good welded joints. The weld bead geometry such as depth of penetration (DP), bead width (BW) and tensile strength (TS) of the laser welded butt joints made of AISI 904L super austenitic stainless steel were investigated. Full factorial design was used to carry out the experimental design. Artificial Neural networks (ANN) program was developed in MatLab software to establish the relationships between the laser welding input parameters like beam power, travel speed and focal position and the three responses DP, BW and TS in three different shielding gases (Argon, Helium and Nitrogen). The established models were used for optimizing the process parameters using Genetic Algorithm (GA). Optimum solutions for the three different gases and their respective responses were obtained (Sathiya et al. 2012).

Bead-on-plate welds were carried out on austenitic stainless steel plates using an electron beam welding machine. Experimental data were collected as per central composite design and regression analysis was conducted to establish input–output relationships of the process. An attempt was made to minimize the weldment area, after satisfying the condition of maximum bead penetration. Thus, it was posed as a constrained optimization problem and solved utilizing a Genetic Algorithm with a penalty function approach. The Genetic Algorithm was able to determine optimal weld-bead geometry and recommend the necessary process parameters for the same (VidyutDeya et al. 2009).

The increasing demand of light weight and durability makes thin-gage galvanized steels (<0.6 mm) attractive for future automotive applications. Laser welding, well known for its deep penetration, high speed

and small heat affected zone, provides a potential solution for welding thin-gage galvanized steels in automotive industry. The effect of the laser welding parameters (i.e. laser power,welding speed, gap and focal position) on the weld bead geometry (i.e. weld depth, weld width and surface concave) of 0.4 mm-thick galvanized SAE1004 steel in a lap joint configuration was investigated by experiments. The process windows of the concerned process parameters were therefore determined. Then, Response Surface Methodology (RSM) was used to develop models to predict the relationship between the processing parameters and the laser weld bead profile and identify the correct and optimal combination of the laser welding input variables to obtain superior weld joint. Under the optimal welding parameters, defect-free weld were produced, and the average aspect ratio increase about 30%, from 0.62 to 0.83 (Yangyang Zhao et al. 2012).

Joining of dissimilar Al–Cu alloy AA2219-T87 and Al–Mg alloy AA5083-H321 plates was carried out using friction stir welding (FSW) technique and the process parameters were optimized using Taguchi L16 orthogonal design of experiments. The rotational speed, transverse speed, tool geometry and ratio between tool shoulder diameter and pin diameter were the parameters taken into consideration. The optimum process parameters were determined with reference to tensile strength of the joint. The predicted optimal value of tensile strength was confirmed by conducting the confirmation run using optimum parameters. The study showed that defect free, high efficiency welded joints can be produced using a wide range of process parameters and recommends parameters for producing best joint tensile properties (Koilraj et al. 2012).

Ranfeng Qiu et al. (2009) joined aluminum alloy A5052 cold-rolled steel plates and austenitic stainless steel SUS304 using resistance spot

welding with a cover plate. They observed interfacial microstructure using transmission electron microscope. Khan et al. (2012) investigated the effects of energy density on geometry of the weld seam and development of microstructures at various weld zones. Energy-based local micro hardness profiles are made and linked with the formation of the microstructures. Weld resistance at the interface is energy-limited and seam profile only changes from conical to cylindrical after a certain limit of energy input. Danial Kianersi et al. (2014) optimized welding parameters namely welding current and time in resistance spot welding of the austenitic stainless steel sheets of grade AISI 304L. They also investigated the effect of optimum welding parameters on the resistance spot welding properties and microstructure of AISI 304L austenitic stainless steel sheets. Tomasz Sadowski et al. (2014) obtained hybrid joints, a combination of two simple techniques, e.g. by spot welding and adhesive, are relatively modern joints developed especially for application in aerospace industry. This contribution describes the modeling and testing of structural elements by application of an angle bar and spot welding techniques with the introduction of adhesive layers between adherents. Timur Canel et al. (2012) investigated the fatigue behavior of resistance spot welding in aluminum 6061-T6 alloy. They included the process optimization of the forces, currents and times for main weld and post-heating. Mustafa Kemal Bilici et al. studied the effects of local electrical contact resistance on transport variables; cooling rate, solute distribution, and nugget shape after solidification responsible for microstructure of the fusion zone during resistance spot welding are realistically and systematically investigated. The model accounts for electromagnetic force, heat generation, contact resistances at the faying surface and electrode work piece interfaces and bulk resistance in work pieces.

RESEARCH GAP

From the above literature survey the following research gap was identified

- Weldability studies of SS304, SS304 & SS304 sheets during TIG and Seam welding using Taguchi technique with L_{27} orthogonal array was not attempted much.
- Few attempts were made on weldability of stainless steel sheets during TIG welding process using Taguchi Technique to accomplish maximum impact strength and hardness.
- Study of seam welding parameters of SS sheets using ANOVA and signal to noise to obtain maximum impact strength and hardness of the joints using Taguchi technique was not attempted much.

CHAPTER 4

RESULTS AND DISCUSSION

WELDABILITY STUDIES ON SEAM WELDING OF SS304

The measured responses are listed in Table 4.1. Design expert 7 software was used for analyzing the measured responses. In this study, an L_{27} orthogonal array with 3 columns and 27 rows was used. Twenty seven experiments were required to study the welding parameters using L_{27} orthogonal array. The responses for signal-to-noise ratio are presented in Table 4.1.

Table 4.1 Response methodology parameters

Exp. No	Input parameters			Response Value		S/N ratio	
	Pressure (Kgf/cm^2)	Speed (rpm)	Temp (°C)	Impact (BHN)	Hardness (J)	Impact	Hardness
1	60	30	40	0.300	83.48	10.4576	-10.4576
2	60	45	50	0.333	67.81	9.5511	-9.5511
3	60	60	60	0.400	80.39	7.9588	-7.9588
4	80	30	40	0.242	82.14	12.3237	-12.3237
5	80	45	50	0.333	86.75	9.5511	-9.5511
6	80	60	60	0.285	91.75	10.9031	-10.9031
7	100	30	40	0.400	89.70	7.9588	-7.9588
8	100	45	50	0.383	91.75	8.3360	-8.3360
9	100	60	60	0.400	68.84	7.9588	-7.9588

Table 4.1 (Continued)

10	100	30	50	0.307	75.07	10.2572	-10.2572
11	100	45	60	0.400	94.95	7.9588	-7.9588
12	100	60	40	0.292	76.25	10.6923	-10.6923
13	60	30	50	0.228	77.87	12.8413	-12.8413
14	60	45	60	0.400	89.70	7.9588	-7.9588
15	60	60	40	0.360	86.75	8.8739	-8.8739
16	80	30	50	0.353	71.31	9.0445	-9.0445
17	80	45	60	0.363	86.75	8.8019	-8.8019
18	80	60	40	0.363	77.87	8.8019	-8.8019
19	80	30	60	0.307	84.86	10.2572	-10.2572
20	80	45	40	0.360	88.21	8.8739	-8.8739
21	80	60	50	0.400	94.95	7.9588	-7.9588
22	100	30	60	0.304	79.12	10.0063	-10.0063
23	100	45	40	0.400	73.91	7.9588	-7.9588
24	100	60	50	0.440	62.41	7.1309	-7.1309
25	60	30	60	0.366	88.21	8.7304	-8.7304
26	60	45	40	0.480	66.81	6.3752	-6.3752
27	60	60	50	0.436	83.48	7.2103	-7.2103

The Signal-to-Noise (S/N) Ratio Analysis

In order to evaluate the influence of each selected factor on the responses: The signal-to-noise ratios S/N for each factor is to be calculated. The signals have indicated that the effect on the average responses and the noises were measured by the influence on the deviations from the average responses, which would indicate the sensitiveness of the experiment output to the noise factors. The appropriate S/N ratio must be chosen using previous knowledge, expertise, and understanding of the process. When the target is

fixed and there is a trivial or absent signal factor (static design), it is possible to choose the S/N ratio depending on the goal of the design. In this study, the S/N ratio was chosen according to the criterion the 'larger is better', in order to maximize the responses. The S/N ratio for the 'larger is better' target for all the responses was calculated as follows,

$$\text{Larger the better: S/N ratio} = -10 \log_{10} \frac{1}{n} \sum_{i=1}^{n} \frac{1}{y_i^2}$$

Using the above presented data with the selected above formula for calculating S/N, the Taguchi experiment results are summarized in Table 4.2 and presented in Figure 4.1 & 4.2, which were obtained by means of MINITAB 13 statistical software. It can be noticed from the figure 4.1 that the S/N plot, the welding speed (S) is the most important factor affecting the impact strength. Welding temperature (T) has a lower effect. Main effects plot for S/N ratios suggest that those levels of variables would increase the impact strength of the weld joint.

Table 4.2 Response table for signal to noise ratios

Level	Pressure (Kgf/cm^2)	Speed (rpm)	Temperature (°C)
1	-8.884	-10.209	-9.146
2	-9.613	-8.374	-9.098
3	-8.695	-8.610	-8.948
Delta	0.198	1.835	0.198
Rank	2	1	3

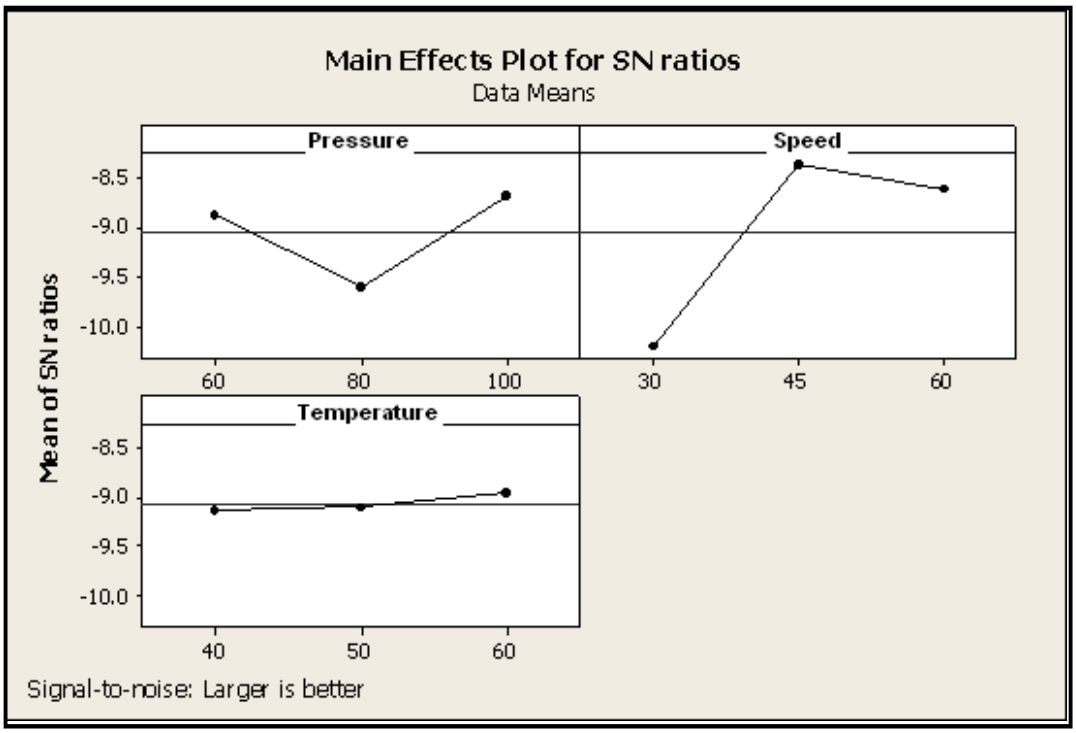

Figure 4.1 Main Effects Plot for SN ratios

From the Figure 4.3 and Table 4.3, it is observed that the welding speed (S) is the most significant factor and the welding temperature (T) is the insignificant factor for the hardness of the weld zone.

Table 4.3 Response table for means

Level	**Pressure Kgf/cm^2**	**Speed rpm**	**Temperature ^{0}C**
1	0.3670	0.3132	0.3552
2	0.3340	0.3836	0.3570
3	0.3709	0.3751	0.3597
Delta	0.0369	0.0703	0.0044
Rank	2	1	3

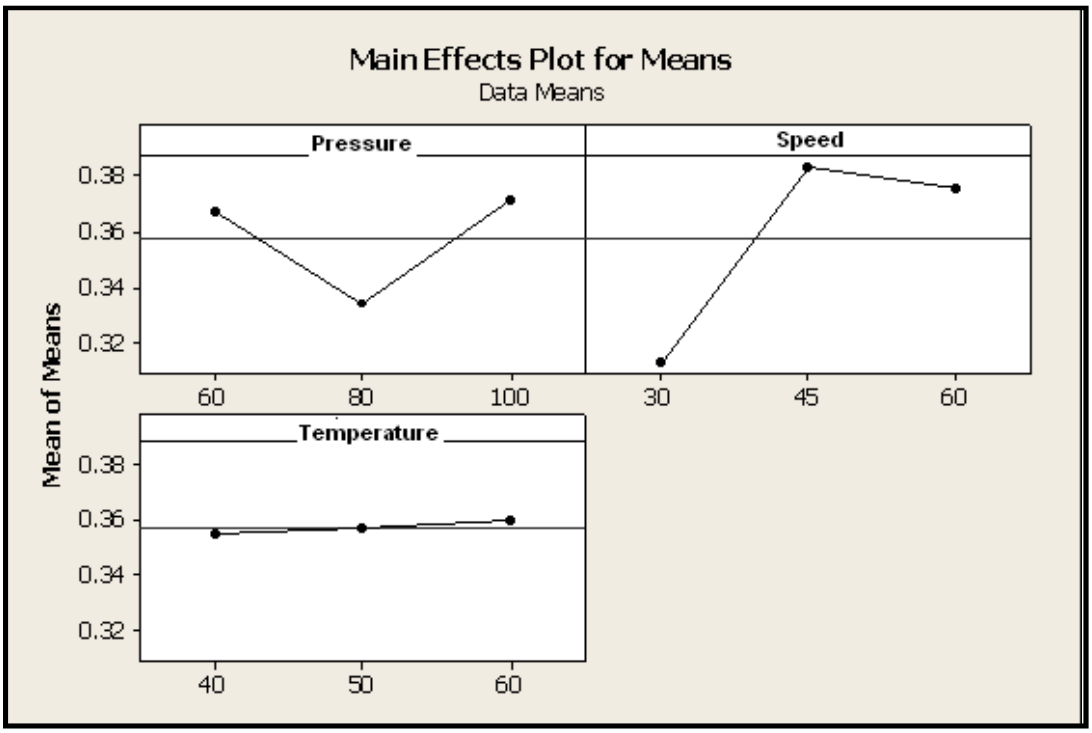

Figure 4.2 Main Effects Plot for Means

Analysis of Variance (ANOVA)

The purpose of the ANOVA is to investigate which welding process parameters significantly affect the quality characteristic. This is accomplished by separating the total variability of the S/N ratios, which is measured by the sum of the squared deviations from the total mean of the S/N ratio, into contributions by each welding process parameter and the error. The percentage contribution by each of the process parameter is the total sum of the squared deviations can be used to evaluate the importance of the process parameter change on the quality characteristic. In addition, the F test can also be used to determine which welding process parameters have a significant effect on the quality characteristic. Usually, the change of the welding process parameter has a significant effect on the quality characteristic when the F value is large.

Analysis of Variance for Impact Strength and Hardness

The purpose of ANOVA is to find the significant factor statistically. It gives a clear picture as to how far the process parameter affects the response and the level of significance of the factor considered. The ANOVA table for mean and signal to noise ratio are calculated and listed in Tables 4.4 and 4.5. The F test is being carried out to study the significance of the process parameter. The high F value indicates that the factor is highly significant in affecting the response of the process. In our investigation, welding speed is a highly significant factor and plays a major role in affecting the impact strength of the weld. Welding temperature is the most significant factor affecting the hardness of weld zone.

Table 4.4 Analysis of variance for impact

Source	DF	SS	MS	F	P
Pressure	2	0.007395	0.003697	1.27	0.303
Speed	2	0.026545	0.013272	4.55	0.024
Temp	2	0.000090	0.000045	0.02	0.985
Error	20	0.058390	0.002919		
Total	26	0.092420			

S = 0.0540323 R-Sq = 36.82% R-Sq(adj) = 17.87%

Table 4.5 Analysis of variance for hardness

Source	DF	SS	MS	F	P
Pressure	2	167.75	83.87	0.97	0.394
Speed	2	32.49	16.25	0.19	0.829
Temp	2	169.32	84.66	0.98	0.391
Error	20	1720.63	86.03		
Total	26	2090.19			

S = 0.0640625 R-Sq = 39.62% R-Sq(adj) = 19.37%

WELDABILITY STUDIES ON TIG WELDING OF SS304

In this study, an L_{27} orthogonal array with 3 columns and 27 rows was used. Twenty seven experiments were required to study the welding parameters using L_{27} orthogonal array. The responses for signal-to-noise ratio are presented in Table 4.6. Design expert 7 software was used for analyzing the measured responses.

Table 4.6 Response methodology parameters

Exp. No	Input parameters			Response Value			S/N ratio		
	Pressure (MPa)	Speed (rpm)	Temp (°C)	Impact	BHN	RHN	Impact	BHN	RHN
1	5.884	30	40	1.157	132.09	94.33	1.157	1.249304	1.249225
2	5.884	45	50	1.21	106.86	75.33	1.21	1.249261	1.249132
3	5.884	60	60	0.956	135.15	72.66	0.956	1.249308	1.249113
4	7.845	30	40	1.091	118.77	87	1.091	4.259482	4.259305
5	7.845	45	50	0.958	152.41	93	0.958	4.259563	4.259353
6	7.845	60	60	0.923	151.65	74	0.923	4.259561	4.259159
7	9.806	30	40	0.767	171.41	85	0.767	5.148977	5.148606
8	9.806	45	50	0.857	144.75	78	0.857	5.148929	5.148514
9	9.806	60	60	0.958	138.21	71.33	0.958	5.148912	5.1484
10	9.806	30	50	0.719	141.38	81.33	0.719	4.259542	4.25925
11	9.806	45	60	0.537	138.15	79	0.537	4.259536	4.259223
12	9.806	60	40	0.961	144.75	94.33	0.961	4.259549	4.259362
13	5.884	30	50	0.821	141.41	84.66	0.821	8.159043	8.158407
14	5.884	45	60	0.706	121.07	73.66	0.706	8.158913	8.158089
15	5.884	60	40	0.667	109.03	81.66	0.667	8.1588	8.158333
16	7.845	30	50	0.828	163.05	93.66	0.828	4.681544	4.6813
17	7.845	45	60	1.263	141.38	80.33	1.263	4.681504	4.68117
18	7.845	60	40	1.09	138.09	82.33	1.09	4.681497	4.681193
19	7.845	30	60	0.885	163.05	86.66	0.885	5.148965	5.148625
20	7.845	45	40	0.786	135.15	76	0.786	5.148904	5.148483
21	7.845	60	50	1.211	123.67	74.33	1.211	5.148866	5.148455
22	9.806	30	60	1.045	100.65	72.33	1.045	4.681349	4.681054
23	9.806	45	40	0.56	185.11	78.33	0.56	4.681571	4.681144
24	9.806	60	50	0.6	151.65	84.66	0.6	4.681525	4.681219
25	5.884	30	60	1.158	148.14	78.33	1.158	9.278717	9.277637
26	5.884	45	40	1.263	126.45	74.66	1.263	9.278561	9.277486
27	5.884	60	50	0.821	159.16	91.33	0.821	9.278773	9.278033

The Signal-to-Noise (SN) Ratio Analysis

In order to evaluate the influence of each selected factor on the responses, The signal-to-noise ratios S/N for each factor is to be calculated. The signals have indicated that the effect on the average responses and the noises were measured by the influence on the deviations from the average responses, which would indicate the sensitiveness of the experiment output to the noise factors. The appropriate S/N ratio must be chosen using previous knowledge, expertise, and understanding of the process. When the target is fixed and there is a trivial or absent signal factor (static design), it is possible to choose the S/N ratio depending on the goal of the design. In this study, the S/N ratio was chosen according to the criterion the 'larger is better', in order to maximize the responses. The S/N ratio for the 'larger is better' target for all the responses was calculated as follows,

$$\text{Larger the better: S/N ratio} = -10 \log_{10} \frac{1}{n} \sum_{i=1}^{n} \frac{1}{y_i^2}$$

where,

n = number of variables

y_i = the value of the response

Using the above presented data with the selected above formula for calculating S/N, the Taguchi experiment results are summarized in Table 4.7 & 4.8 and presented in Figure 4.3 & 4.4, which were obtained by means of MINITAB 15 statistical software. It can be noticed from the figure 4.3 (the S/N plot), the welding pressure (P) is the most important factor affecting the impact strength. Welding temperature (T) has a lower effect. Main effects plot for S/N ratios suggest that those levels of variables would increase the impact strength of the weld joint.

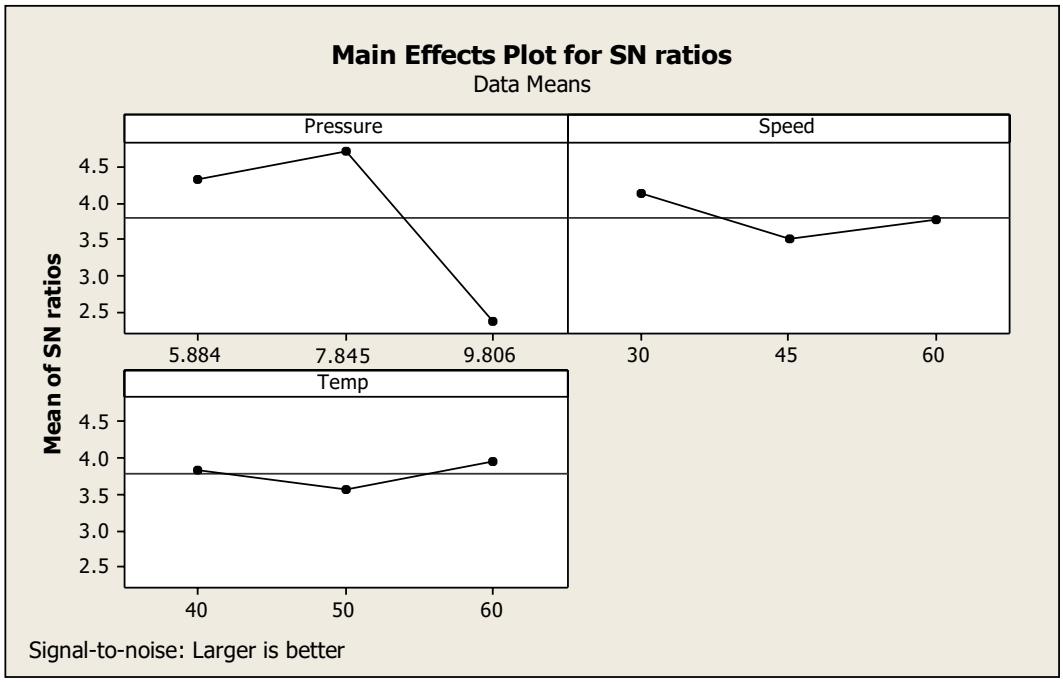

Figure 4.3 Main effects plot for S/N ratios

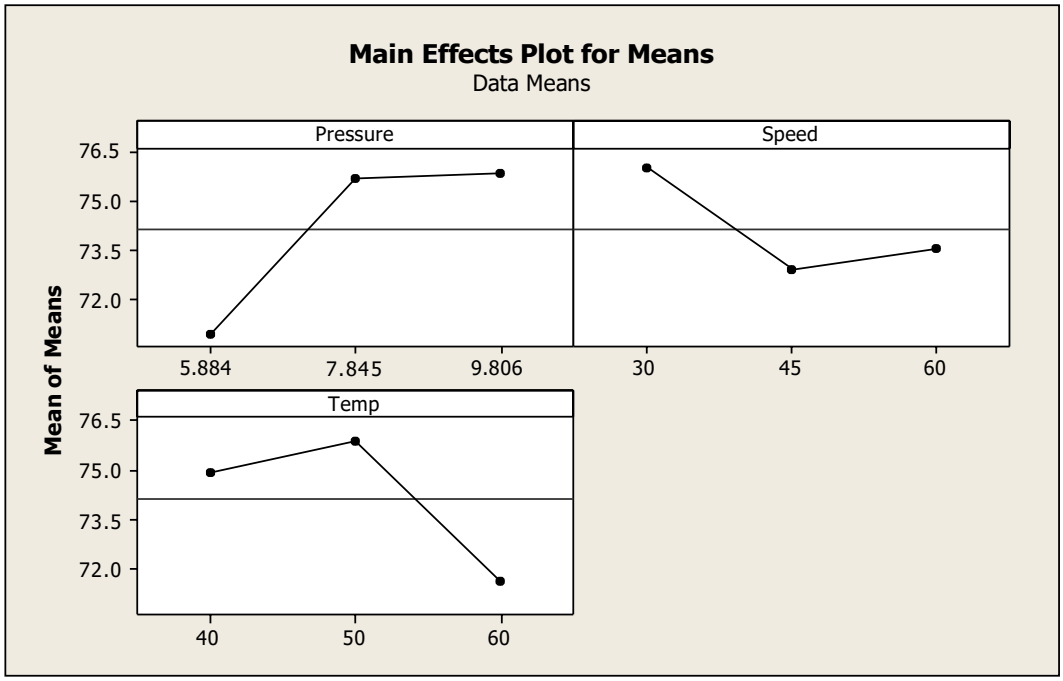

Figure 4.4 Main effects plot for means

Table 4.7 Response table for S/N ratios

Level	Pressure MPa	Speed Rpm	Temperature ^{0}C
1	4.311	4.114	3.827
2	4.696	3.487	3.575
3	2.357	3.764	3.964
Delta	2.339	0.628	0.389
Rank	1	2	3

Table 4.8 Response table for means

Level	Pressure MPa	Speed Rpm	Temperature ^{0}C
1	70.92	75.99	74.92
2	75.69	72.88	75.88
3	75.83	73.56	71.64
Delta	4.91	3.11	4.24
Rank	1	3	2

Interaction Plot for SN Ratio

From the interaction plot shown in figure 4.5, it is observed that the interaction of S/N ratio, the pressure value increases with respect to temperature. The S/N ratio value increases with the increase in speed for moderate temperature.

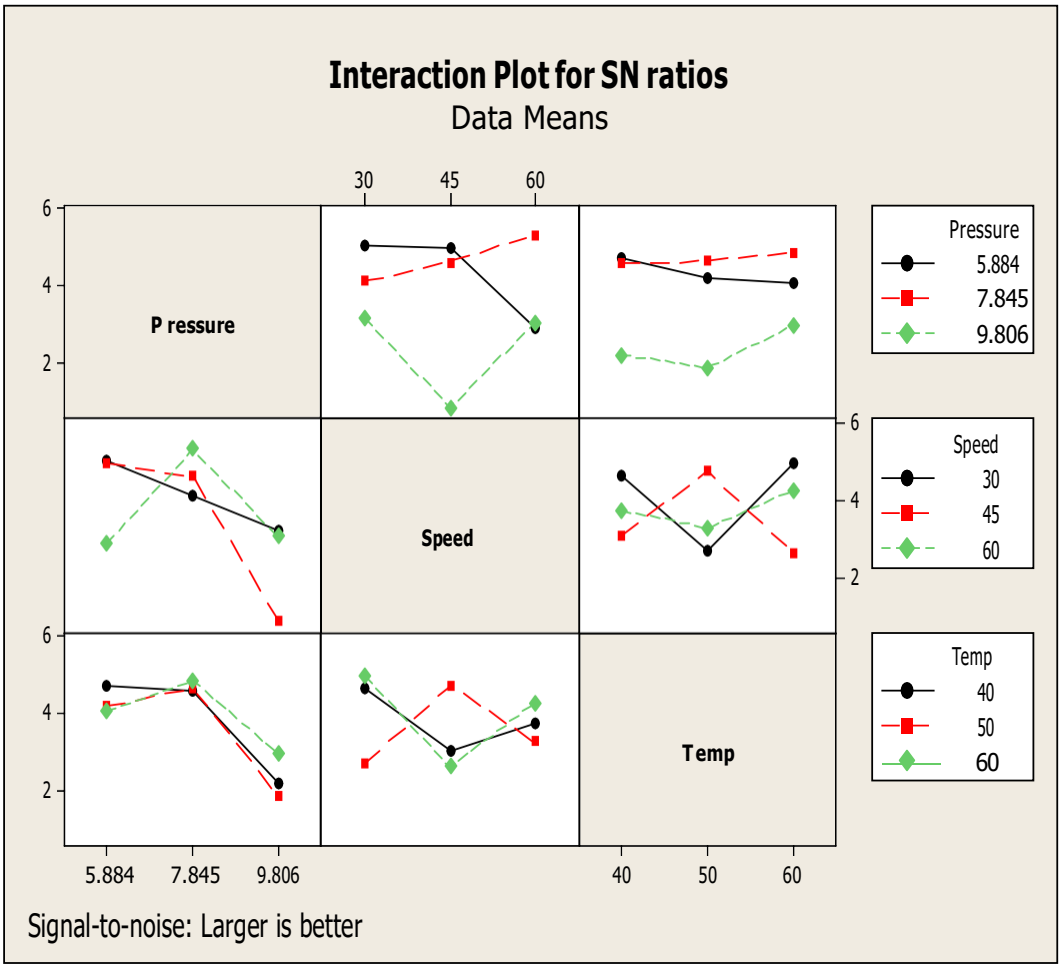

Figure 4.5 Interaction plot for SN ratios

Analysis of Variance (ANOVA)

The purpose of the ANOVA is to investigate which welding process parameters significantly affect the quality characteristic. This is accomplished by separating the total variability of the S/N ratios, which is measured by the sum of the squared deviations from the total mean of the S/N ratio, contributions by each welding process parameter and the error. The percentage contribution by each of the process parameter is the total sum of the squared deviations which is used to evaluate the importance of the process parameter change on the quality characteristic. In addition, the F test can also be used to determine which welding process parameters have a significant

effect on the quality characteristic. Usually, the change of the welding process parameter has a significant effect on the quality characteristic when the F value is large.

Analysis of Variance for Impact Strength and Hardness (BHN, RHN)

The purpose of ANOVA is to find the significant factor statistically. It gives a clear picture as to how far the process parameter affects the response and the level of significance of the factor considered. The ANOVA table for mean and signal to noise ratio are calculated and listed in Tables 4.9, 4.10 and 4.11. The F test is being carried out to study the significance of the process parameter. The high F value indicates that the factor is highly significant in affecting the response of the process. In our investigation, welding speed is a highly significant factor and plays a major role in affecting the impact strength of the weld. Welding temperature is the most significant factor affecting the hardness of weld zone.

Table 4.9 Analysis of variance for impact

Source	DF	SS	MS	F	P
Pressure	2	0.007595	0.003689	1.25	0.303
Speed	2	0.026515	0.013270	4.45	0.024
Temp	2	0.000070	0.000047	0.03	0.985
Error	20	0.056390	0.002918		
Total	26	0.092520			

S = 0.0540323 R-Sq = 36.82% R-Sq (adj) = 17.87%

Table 4.10 Analysis of variance for BHN

Source	DF	SS	MS	F	P
Pressure	2	168.75	83.86	0.96	0.394
Speed	2	32.49	16.27	0.18	0.829
Temp	2	168.32	84.65	0.97	0.391
Error	20	1710.63	86.07		
Total	26	2096.19			

S = 0.0640625 R-Sq = 39.62% R-Sq(adj) = 19.37%

Table 4.11 Analysis of variance for RHN

Source	DF	SS	MS	F	P
Pressure	2	169.75	83.86	0.95	0.393
Speed	2	32.49	16.27	0.18	0.827
Temp	2	168.33	85.64	0.97	0.399
Error	20	1710.63	86.07		
Total	26	2195.19			

S = 0.0750623 R-Sq = 40.66% R-Sq(adj) = 20.52%

WELDABILITY STUDIES ON SEAM WELDING OF SS304

In this study, an L_{27} orthogonal array with 3 columns and 27 rows was used. Twenty seven experiments were required to study the welding parameters using L_{27} orthogonal array. The responses for signal-to-noise ratio are presented in Table 4.12. Design expert 7 software was used for analyzing the measured responses.

Table 4.12 Response methodology parameters

Experiment No	Input parameters			Response Value			S/N ratio		
	Pressure (MPa)	Speed (rpm)	Temperature (°C)	Impact	BHN	RHN	Impact	BHN	RHN
1	5.884	30	40	1.071	109.03	87.67	1.071	132.09	1.249199
2	5.884	45	50	1.071	106.86	77.0	1.071	106.86	1.249143
3	5.884	60	60	1.071	111.34	87.33	1.071	111.34	1.249198
4	7.845	30	40	1.191	106.86	86.67	1.191	106.86	4.259302
5	7.845	45	50	1.191	126.45	82.0	1.191	126.45	4.259257
6	7.845	60	60	1.131	106.86	82.33	1.131	106.86	4.25926
7	9.806	30	40	1.191	104.75	81.67	1.191	104.75	5.148565
8	9.806	45	50	1.071	109.03	94	1.071	109.03	5.148696
9	9.806	60	60	1.191	121.07	82.33	1.191	121.07	5.148574
10	9.806	30	50	1.071	100.65	78	1.071	100.65	4.259211
11	9.806	45	60	1.071	83.35	80.33	1.071	83.35	4.259239
12	9.806	60	40	1.191	129.23	75.33	1.191	129.23	4.259177
13	5.884	30	50	1.071	109.03	85.67	1.071	109.03	8.15843
14	5.884	45	60	1.131	118.46	74.67	1.131	118.46	8.158124
15	5.884	60	40	1.191	121.07	79.33	1.191	121.07	8.158269
16	7.845	30	50	1.131	106.86	74.67	1.131	106.09	4.681092
17	7.845	45	60	1.071	100.65	86.67	1.071	100.65	4.681239
18	7.845	60	40	1.071	129.23	84.67	1.071	129.23	4.681219
19	7.845	30	60	1.071	109.03	85.33	1.071	109.03	5.14861
20	7.845	45	40	1.071	96.78	82.33	1.071	96.78	5.148574
21	7.845	60	50	1.131	94.95	79.33	1.131	94.95	5.148653
22	9.806	30	60	1.071	89.70	85.33	1.071	89.7	4.681226
23	9.806	45	40	1.191	118.02	84.0	1.191	118.46	4.681212
24	9.806	60	50	1.071	116.02	85.33	1.071	116.02	4.681226
25	5.884	30	60	1.131	104.75	83.67	1.131	104.75	9.277822
26	5.884	45	40	1.131	118.46	81.67	1.131	118.46	9.277757
27	5.884	60	50	1.071	106.86	77.67	1.071	106.86	9.277611

The Signal-to-Noise (S/N) Ratio Analysis

In order to evaluate the influence of each selected factor on the responses, The signal-to-noise ratios S/N for each factor is to be calculated. The signals have indicated that the effect on the average responses and the noises were measured by the influence on the deviations from the average responses, which would indicate the sensitiveness of the experiment output to the noise factors. The appropriate S/N ratio must be chosen using previous knowledge, expertise, and understanding of the process. When the target is fixed and there is a trivial or absent signal factor (static design), it is possible to choose the S/N ratio depending on the goal of the design. In this study, the S/N ratio was chosen according to the criterion the 'larger is better', in order to maximize the responses. The S/N ratio for the 'larger is better' target for all the responses was calculated as follows,

$$\text{Larger the better: S/N ratio} = -10 \log \frac{1}{n} \sum_{i=1}^{n} \frac{1}{y_i^2}$$

where,

n = number of variables

y_i = the value of the response

Using the above presented data with the selected above formula for calculating S/N, the Taguchi experiment results are summarized in Table 4.13 & 4.14 and presented in Figure 4.6 & 4.7, which were obtained by means of MINITAB 15 statistical software. It can be noticed from the figure 4.6 (the S/N plot), the welding temperature (T) is the most important factor affecting the impact strength. Welding speed (S) has a lower effect. Main effects plot for S/N ratios suggest that those levels of variables would increase the impact strength of the weld joint.

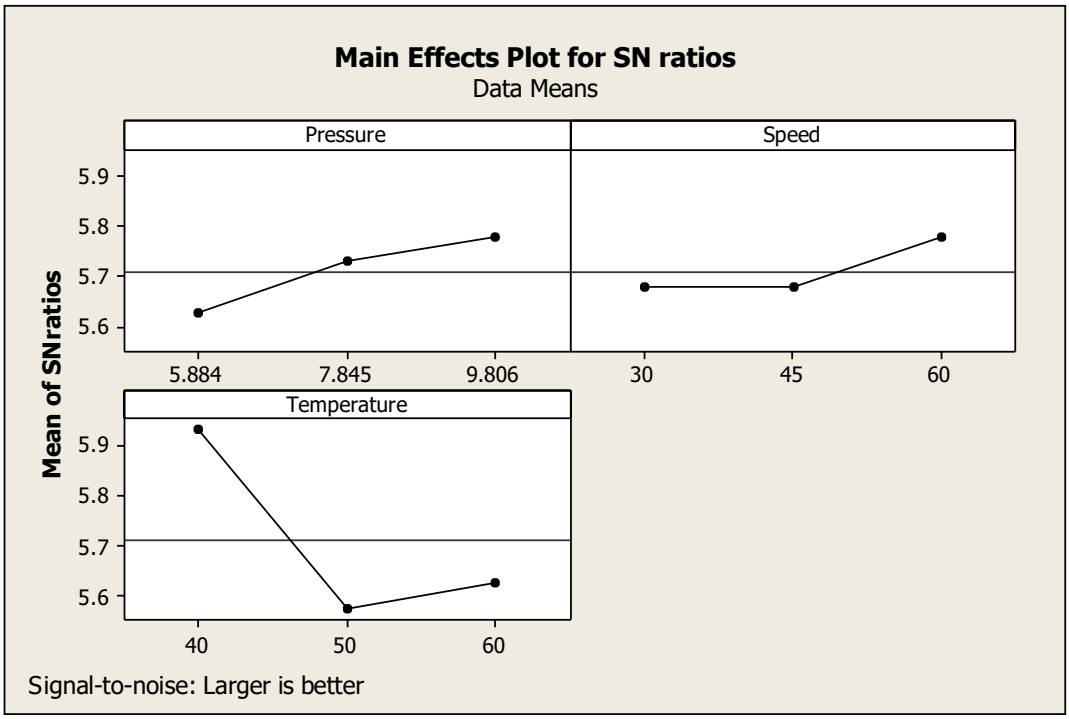

Figure 4.6 Main effects plot for S/N ratios

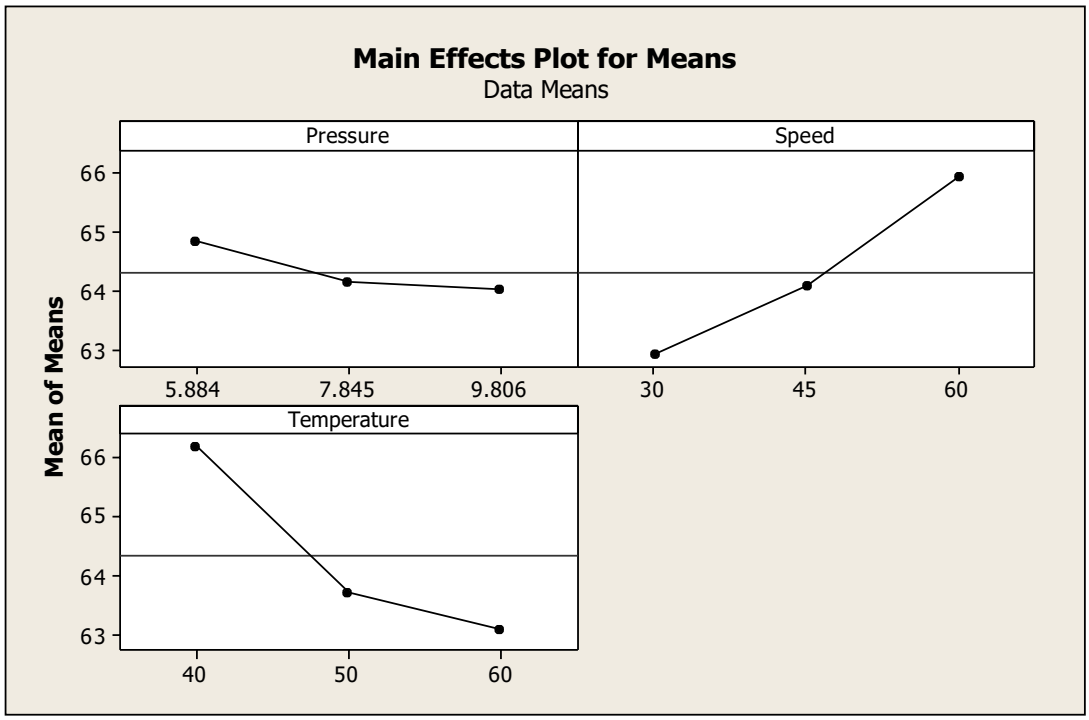

Figure 4.7 Main effects plot for means

Table 4.13 Response table for S/N ratios

Level	Pressure MPa	Speed Rpm	Temperature ^{0}C
1	5.626	5.676	5.931
2	5.729	5.676	5.573
3	5.776	5.778	5.626
Delta	0.150	0.103	0.357
Rank	2	3	1

Table 4.14 Response table for means

Level	Pressure MPa	Speed Rpm	Temp ^{0}C
1	64.83	62.94	66.19
2	64.14	64.10	63.71
3	64.01	65.94	63.08
Delta	0.82	3.00	3.11
Rank	3	2	1

Interaction Plot for SN ratio

From the interaction plot shown in Figure 4.8, it is observed that the interaction of S/N ratio, the temperature value increases with respect to pressure. The S/N ratio value increases with the increase in pressure for moderate speed.

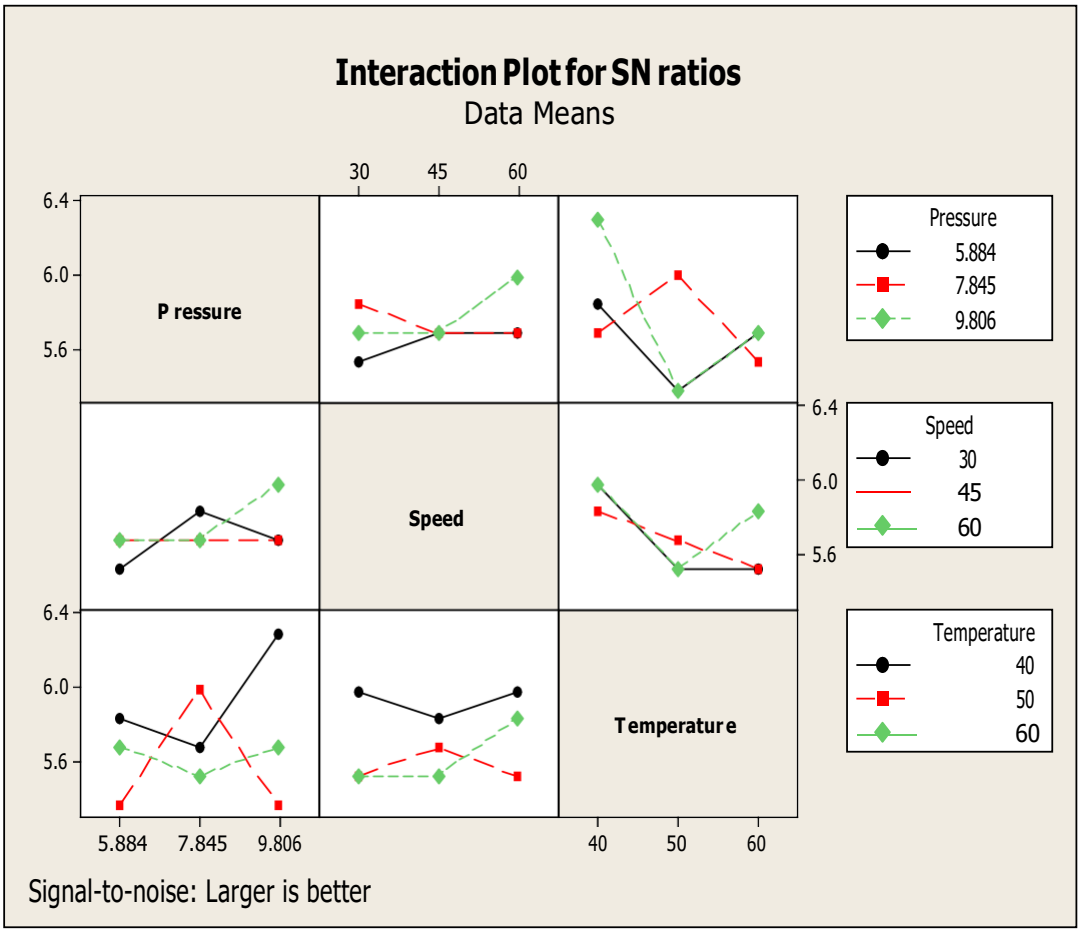

Figure 4.8 Interaction plot for S/N ratios

Analysis of Variance (ANOVA)

The purpose of the ANOVA is to investigate which welding process parameters significantly affect the quality characteristic. This is accomplished by separating the total variability of the S/N ratios, which is measured by the sum of the squared deviations from the total mean of the S/N ratio, into contributions by each welding process parameter and the error. The percentage contribution by each of the process parameter is the total sum of the squared deviations can be used to evaluate the importance of the process parameter change on the quality characteristic. In addition, the F test can also be used to determine which welding process parameters have a significant

effect on the quality characteristic. Usually, the change of the welding process parameter has a significant effect on the quality characteristic when the F value is large.

Analysis of Variance for Impact Strength and Hardness (BHN, RHN)

The purpose of ANOVA is to find the significant factor statistically. It gives a clear picture as to how far the process parameter affects the response and the level of significance of the factor considered. The ANOVA table for mean and signal to noise ratio are calculated and listed in Tables 4.15, 4.16 and 4.17. The F test is being carried out to study the significance of the process parameter. The high F value indicates that the factor is highly significant in affecting the response of the process. In our investigation, welding speed is a highly significant factor and plays a major role in affecting the impact strength of the weld. Welding temperature is the most significant factor affecting the hardness of weld zone.

Table 4.15 Analysis of variance for impact

Source	DF	SS	MS	F	P
Pressure	2	0.006685	0.003610	1.33	0.378
Speed	2	0.026765	0.013498	4.41	0.031
Temperature	2	0.000059	0.000039	0.03	0.898
Error	20	0.056408	0.002912		
Total	26	0.093654			

S = 0.0540543 R-Sq = 34.23% R-Sq (adj) = 15.45%

Table 4.16 Analysis of variance for BHN

Source	DF	SS	MS	F	P
Pressure	2	166.78	82.65	0.91	0.376
Speed	2	31.98	16.67	0.21	0.879
Temperature	2	166.91	83.89	0.96	0.354
Error	20	1708.78	85.98		
Total	26	2098.11			

S = 0.0630765 R-Sq = 38.78% R-Sq (adj) = 18.78%

Table 4.17 Analysis of variance for RHN

Source	DF	SS	MS	F	P
Pressure	2	168.55	82.99	0.98	0.373
Speed	2	31.88	16.98	0.18	0.846
Temp	2	166.45	85.45	0.95	0.345
Error	20	1767.89	86.45		
Total	26	2187.54			

S = 0.0750808 R-Sq = 39.87% R-Sq(adj) = 29.95%

WELDABILITY STUDIES ON TIG WELDING OF SS304

In this study, an L_{27} orthogonal array with 3 columns and 27 rows was used. Twenty seven experiments were required to study the welding parameters using L_{27} orthogonal array. The responses for signal-to-noise ratio are presented in Table 4.18. Design expert 7 software was used for analyzing the measured responses.

Table 4.18 Response methodology parameters

Experiment No	Input parameters			Response Value			SN ratio		
	Pressure (MPa)	Speed (rpm)	Temperature (°C)	Impact	BHN	RHN	Impact	BHN	RHN
1	5.884	30	40	1.071	132.09	65.66	0.14146	1.249304	1.249052
2	5.884	45	50	1.071	106.86	71.66	0.14146	1.249261	1.249105
3	5.884	60	60	1.071	135.15	88.66	0.14146	1.249308	1.249203
4	7.845	30	40	1.191	118.77	75	2.58655	4.259482	4.259173
5	7.845	45	50	1.191	152.41	78.33	2.58655	4.259563	4.259215
6	7.845	60	60	1.131	151.65	72.66	2.4379	4.259561	4.259139
7	9.806	30	40	1.191	171.41	74	3.17133	5.148977	5.148449
8	9.806	45	50	1.071	144.75	88.66	2.81077	5.148929	5.148646
9	9.806	60	60	1.191	138.21	73.33	3.17133	5.148912	5.148437
10	9.806	30	50	1.071	141.38	81.33	2.2698	4.259542	4.25925
11	9.806	45	60	1.071	135.15	79.33	2.2698	4.259529	4.259227
12	9.806	60	40	1.191	144.75	72.22	2.58655	4.259549	4.259132
13	5.884	30	50	1.071	141.41	68	4.30942	8.159043	8.157861
14	5.884	45	60	1.131	121.07	72.66	4.58148	8.158913	8.158052
15	5.884	60	40	1.191	109.03	72.66	4.82774	8.1588	8.158052
16	7.845	30	50	1.131	163.05	67.33	2.71063	4.681544	4.68096
17	7.845	45	60	1.071	141.38	80.66	2.53187	4.681504	4.681174
18	7.845	60	40	1.071	132.09	83.33	2.53187	4.681481	4.681205
19	7.845	30	60	1.071	163.05	71.66	2.81077	5.148965	5.148406
20	7.845	45	40	1.071	135.15	72.66	2.81077	5.148904	5.148425
21	7.845	60	50	1.131	123.67	66	3.00166	5.148866	5.148283
22	9.806	30	60	1.071	100.65	77.33	2.53187	4.681349	4.681131
23	9.806	45	40	1.191	185.11	71.66	2.86911	4.681571	4.681043
24	9.806	60	50	1.071	151.65	78.66	2.53187	4.681525	4.681148
25	5.884	30	60	1.131	148.14	66	5.03768	9.278717	9.277025
26	5.884	45	40	1.131	126.45	84.66	5.03768	9.278561	9.277853
27	5.884	60	50	1.071	159.16	79.33	4.73651	9.278773	9.277675

The Signal-to-Noise (SN) Ratio Analysis

In order to evaluate the influence of each selected factor on the responses, The signal-to-noise ratios S/N for each factor is to be calculated. The signals have indicated that the effect on the average responses and the noises were measured by the influence on the deviations from the average responses, which would indicate the sensitiveness of the experiment output to the noise factors. The appropriate S/N ratio must be chosen using previous knowledge, expertise, and understanding of the process. When the target is fixed and there is a trivial or absent signal factor (static design), it is possible to choose the S/N ratio depending on the goal of the design. In this study, the S/N ratio was chosen according to the criterion the 'larger is better', in order to maximize the responses. The S/N ratio for the 'larger is better' target for all the responses was calculated as follows,

$$\text{Larger the better: S/N ratio} = -10 \log_{10} \frac{1}{n} \sum_{i=1}^{n} \frac{1}{y_i^2}$$

where,

n = number of variables

yi = the value of the response

Using the above presented data with the selected above formula for calculating S/N, the Taguchi experiment results are summarized in Table 4.19 & 4.20 and presented in Figure 4.9 & 4.10, which were obtained by means of MINITAB 15 statistical software. Main effects plot for S/N ratios suggest that those levels of variables would increase the impact strength of the weld joint.

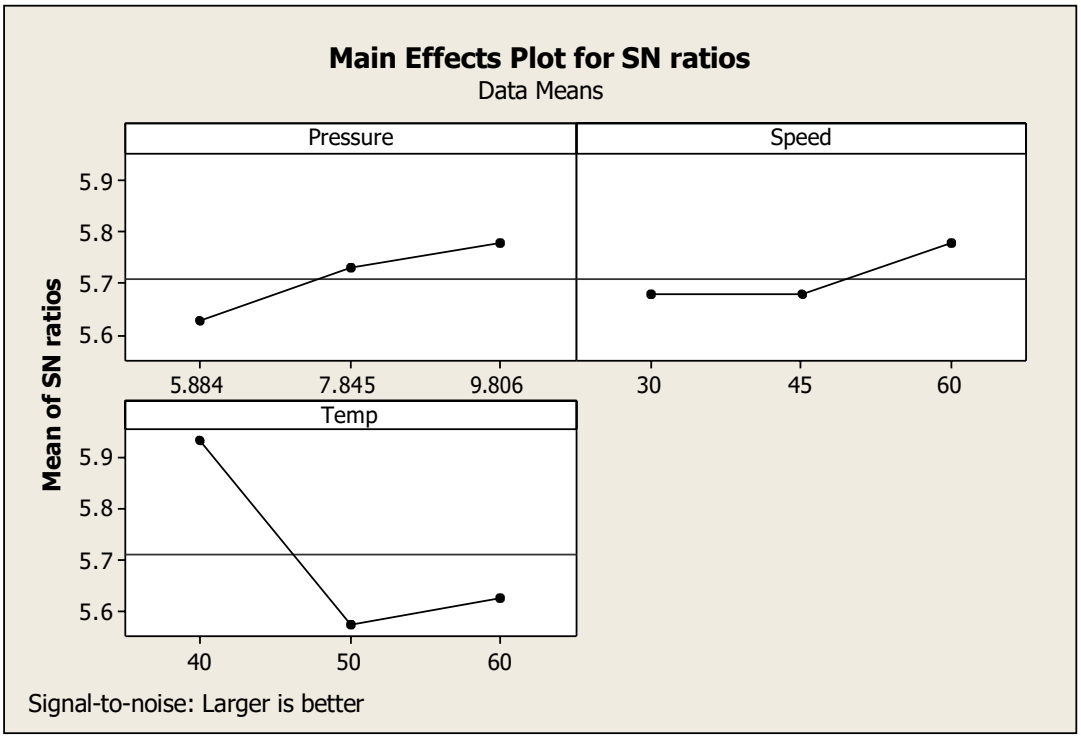

Figure 4.9 Main effects plot for S/N ratios

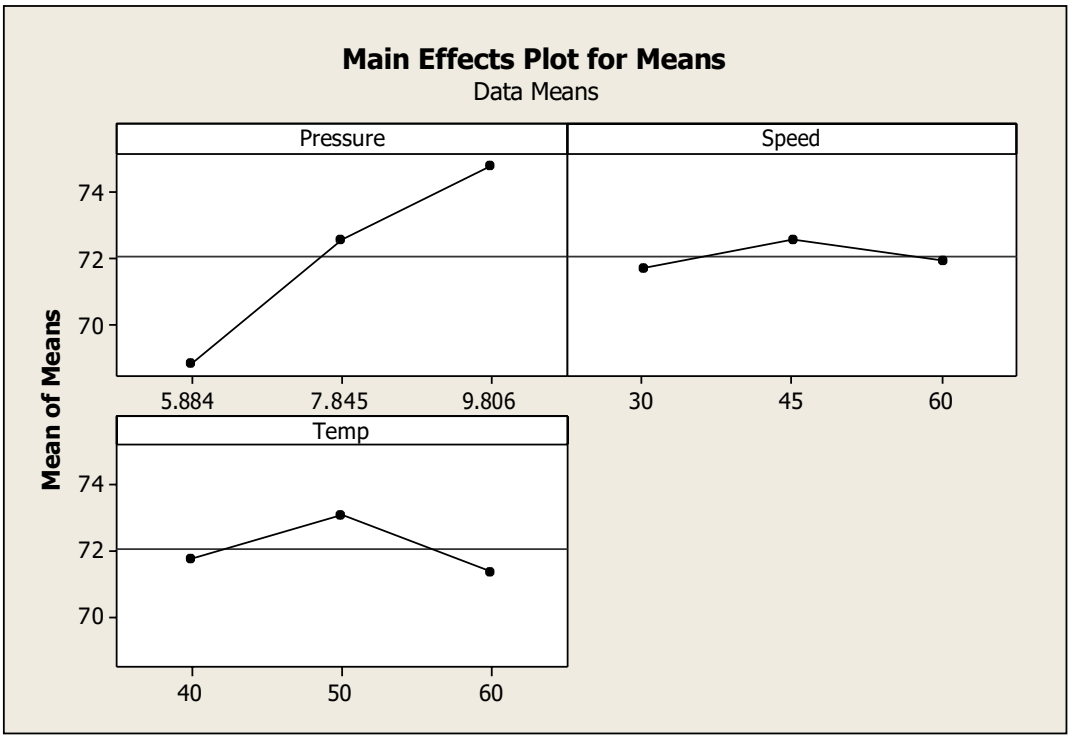

Figure 4.10 Main effects plot for means

Table 4.19 Response table for S/N ratios

Level	Pressure MPa	Speed Rpm	Temperature ^{0}C
1	5.626	5.676	5.931
2	5.729	5.676	5.573
3	5.778	5.778	5.626
Delta	0.150	0.103	0.357
Rank	2	3	1

Table 4.20 Response table for means

Level	Pressure MPa	Speed Rpm	Temperature ^{0}C
1	68.84	71.71	71.74
2	72.55	72.54	73.09
3	74.80	71.94	71.36
Delta	5.97	0.83	1.73
Rank	1	3	2

Interaction Plot for S/N ratio

From the interaction plot shown in figure 4.11, it is observed that the interaction of S/N ratio, the pressure value increases with respect to temperature. The S/N ratio value increases with the increase in speed for moderate temperature.

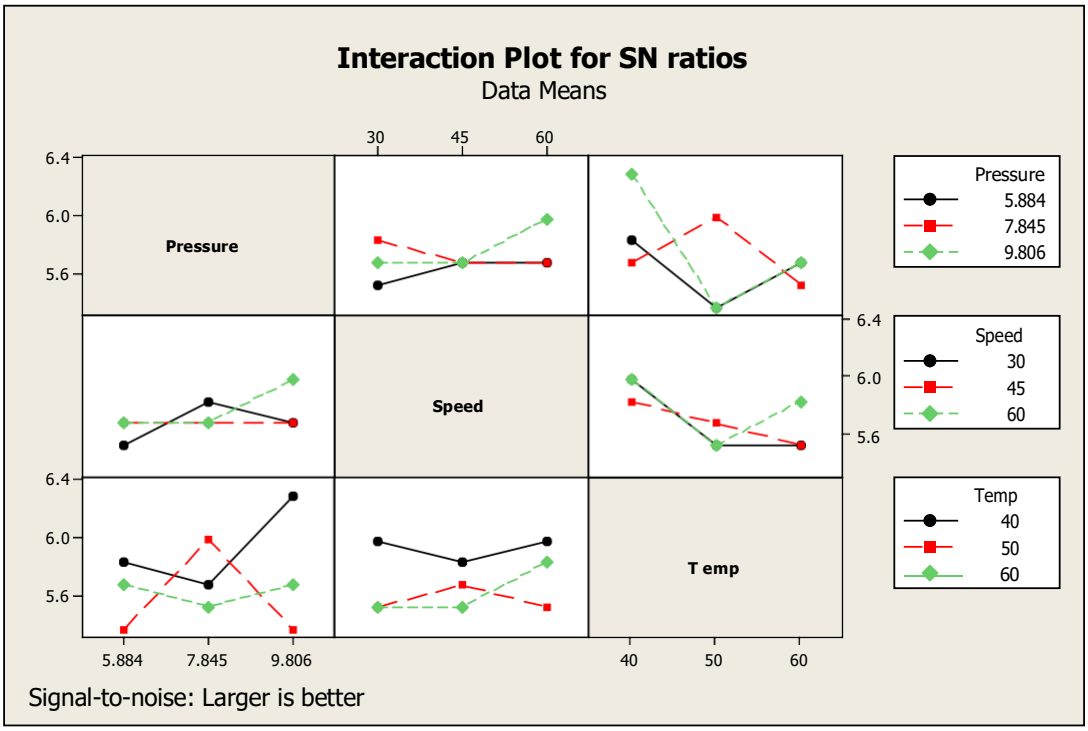

Figure 4.11 Interaction plot for S/N ratios

Analysis of Variance (ANOVA)

The purpose of the ANOVA is to investigate which welding process parameters significantly affect the quality characteristic. This is accomplished by separating the total variability of the SN ratios, which is measured by the sum of the squared deviations from the total mean of the S/N ratio, contributions by each welding process parameter and the error. The percentage contribution by each of the process parameter is the total sum of the squared deviations which is used to evaluate the importance of the process parameter change on the quality characteristic. In addition, the F test can also be used to determine which welding process parameters have a significant effect on the quality characteristic. Usually, the change of the welding process parameter has a significant effect on the quality characteristic when the F value is large.

Analysis of Variance for Impact Strength and Hardness (BHN, RHN)

The purpose of ANOVA is to find the significant factor statistically. It gives a clear picture as to how far the process parameter affects the response and the level of significance of the factor considered. The ANOVA table for mean and signal to noise ratio are calculated and listed in Tables 4.21, 4.22 and 4.23. The F test is being carried out to study the significance of the process parameter. The high F value indicates that the factor is highly significant in affecting the response of the process. In our investigation, welding speed is a highly significant factor and plays a major role in affecting the impact strength of the weld. Welding temperature is the most significant factor affecting the hardness of weld zone.

Table 4.21 Analysis of variance for impact

Source	DF	SS	MS	F	P
Pressure	2	0.006595	0.003579	1.23	0.302
Speed	2	0.026613	0.013350	4.39	0.026
Temperature	2	0.000060	0.000041	0.03	0.974
Error	20	0.056380	0.002865		
Total	26	0.093520			

S = 0.0540412 R-Sq = 35.45% R-Sq (adj) = 16.75%

Table 4.22 Analysis of variance for BHN

Source	DF	SS	MS	F	P
Pressure	2	167.96	83.54	0.97	0.367
Speed	2	32.53	16.87	0.19	0.887
Temperature	2	167.98	84.85	0.97	0.369
Error	20	1702.54	86.35		
Total	26	2085.43			

S = 0.0630689 R-Sq = 38.45% R-Sq (adj) = 18.76%

Table 4.23 Analysis of variance for RHN

Source	DF	SS	MS	F	P
Pressure	2	168.67	83.97	0.94	0.376
Speed	2	32.86	16.65	0.19	0.837
Temperature	2	167.87	85.25	0.96	0.354
Error	20	1723.98	86.98		
Total	26	2194.54			

S = 0.0750785 R-Sq = 40.27% R-Sq(adj) = 20.95%

CHAPTER 5

CONCLUSION AND FUTURE WORK

5. 1 CONCLUSION

The following conclusions were drawn from the analysis of Experimental data and various parameters determined in the present investigation.

Weldability of SS304 Sheets

- The stainless steel sheets (304 Grade) are joined successfully using resistance seam welding process.
- Welding speed influences most on the impact strength of the weld joint among the selected parameters.
- Weld zone hardness is affected by the factor of welding temperature during seam welding of stainless steel sheets.
- Taguchi's design method can be effectively used for optimizing the welding parameters.

Weldability of SS304 Sheets

- The stainless steel sheets (304 Grade) are joined successfully using TIG welding process.

- Welding pressure influences most on the impact strength of the weld joint among the selected parameters.
- Weld zone hardness is affected by the factor of welding temperature during TIG welding of stainless steel sheets.
- Taguchi's design method can be effectively used for optimizing the welding parameters.

Weldability of SS304 Sheets

- The stainless steel sheets (304 Grade) are joined successfully using Seam welding process.
- Welding speed influences most on the impact strength of the weld joint among the selected parameters.
- Weld zone hardness is affected by the factor of welding temperature during Seam welding of stainless steel sheets.
- Taguchi's design method can be effectively used for optimizing the welding parameters.
- The stainless steel sheets (304 Grade) are joined successfully using TIG welding process.
- Welding speed influences most on the impact strength of the weld joint among the selected parameters.
- Weld zone hardness is affected by the factor of welding temperature during TIG welding of stainless steel sheets.
- Taguchi's design method can be effectively used for optimizing the welding parameters.

5. 2 SCOPE FOR FUTURE WORK

- TIG weldability of SS304, SS304 and SS304 can be studied using nontraditional optimisation technique such as Genetic Algorithm, Particle Swarm etc.,
- Seam & TIG welding parameters can be optimized to achieve maximum tensile strength of joints.
- Weldability studies on SS304, SS304 and SS304 stainless sheets during Seam welding can be analyzed using nontraditional optimisation technique such as Genetic Algorithm, Particle Swarm etc.,

LIMITATIONS OF THIS RESEARCH

The following are the limitations of this research,

- Welding parameters were not optimized using non-traditional optimization technique. Only Taguchi Technique was employed.
- Tensile test of the specimens are not carried out during this research.
- Weld defects were not analyzed in the entire study.
- Microstructural analysis of the weldment is not carried out in this study.

REFERENCES

1. Alaa Muhsin Saeed, Zuhailawati Hussain, Ahmad Badri & Tadashi Ariga 2010, 'The effects of welding parameters on the weldability of different materials using brazing alloy fillers', Materials and Design, vol.31, pp. 3339-3345.

2. Ammar Azeez Mahdi, Salih Kareem Waheed & Abdul Wahab Hassan Khuder 2013, 'Effect Of Adding Copper Foils On Seam Welding Joints of 304 Austenitic Stainless Steel', Diyala Journal Engineering Science', vol.7 pp.80-91.

3. Anawa, EM & Olabi, AG 2008, 'Using Taguchi method to optimize welding pool of dissimilar laser-welded components', Optics & Laser Technology, vol. 40, pp.379-388.

4. Bappa Acherjee, Arunanshu S Kuar, Souren Mitra & Dipten Misra 2012, 'Modeling and analysis of simultaneous laser transmission welding of polycarbonates using an FEM and RSM combined approach Optics & Laser Technology vol. 44, pp.995-1006.

5. Bates, PJ, Mahb, JC, Zoub, XP, Wangb, CY & Bobbye Baylis 2004, 'Vibration welding air intake manifolds from reinforced nylon 66,nylon 6 and polypropylene', Composites, vol.35, pp.1107-1116.

6. Bekir S Yilba, Ahmet Z Sahin , Nafiz Kahraman & Ahmed Z A1-Garni 1995, 'Friction welding of St-A1 and A1-Cu materials', Journal of Materials Processing Technology, vol. 49. pp. 431-443 .

7. Benyounis, KY, Olabi, AG & Hashmi, MSJ 2005, 'Effect of laser welding parameters on the heat input and weld-bead profile', Journal of Materials Processing Technology, vol.164-165, pp.978-985.

8. Bingol, S & Keskin, MS 2007, 'A quality problem in seam welds in aluminum extrusion', Archives of Materials Science and Engineering, vol. 28 pp.397-400.

9. Bingol, S, Keskin, MS & Bozac, A 2007, 'Properties of seam welds produced with different extrusion parameters' Archives of Materials Science and Engineering, vol. 28, pp. 365-368

10. Cao, X, Wanjara, P, Huang, J, Munro, bC & Nolting, A 2011, 'Hybrid fiber laser – Arc welding of thick section high strength low alloy steel', Materials and Design, vol. 32, pp.3399-3413.

11. Danial Kianersi, Amir Mostafaei & Ahmad Ali Amadeh 2014, 'Resistance spot welding joints of AISI 304L austenitic stainless steel sheets: Phase transformations, mechanical properties and microstructure characterizations', Mater. Design. DOI:10.1016/j.matdes.2014.04.075, vol. 61, pp. 251-263.

12. Del Coz Díaz, JJ, Menendez Rodriguez, P, Garcia Nieto, PJ, Castro-Fresno, D 2010, 'Comparative analysis of TIG welding distortions between austenitic and duplex stainless steels by FEM,' Applied Thermal Engineering, vol. 30, pp. 2448-2459.

13. Dongjie Li, Shanping Lu, Wenchao Dong, Dianzhong Li & Yiyi Li 2012, 'Study of the law between the weld pool shape variations with the welding parameters under two TIG Processes', Journal of Materials Processing Technology, vol. 212, pp. 128-136.

14. Dube, M, Hubert, P, Yousefpour, A & Denault, J 2007, 'Resistance welding of thermoplastic composites skin/stringer joints', Composites, vol. 38, pp. 2541-2552.

15. Elena Koleva 2001, 'Statistical modelling and computer programs for optimization of the electron beam welding of stainless steel', Institute of Electronics', Bulgarian Academy of Sciences, vol. 72, pp.151-157.

16. Goes, KC, Batalha, GF, Pereira, MV & Camarao, AF 2011, 'Practical methodology to evaluate the fatigue life of seam welded joints', Journal of Achievements in Materials and Manufacturing Engineering, vol.49, pp.35-41.

17. Her-Yueh Huang 2010, 'Effects of activating flux on the welded joint characteristics in gas metal arc welding', Materials and Design vol.31, pp. 2488-2495.

18. Hongmei Li, Daqian Sun, Xiaolong Cai, Peng Dong & Xiaoyan Gu 2013, 'Laser welding of TiNi shape memory alloy and stainless steel using Co filler metal', Optics & Laser Technology, vol. 45, pp.453-460.

19. Hongxin Shi, Ranfeng Qiu, Jinhong Zhu, Keke Zhang Hua Yu & Gaojian Ding 2010, 'Effects of welding parameters on the characteristics of magnesium alloy join welded by resistance spot welding with cover plates', Materials and Design, vol. 31, pp. 4853-4857.

20. Ill-Soo Kim & oon-Sik SonPrasad KDV Yarlagadda 2003, 'A study on the quality improvement of robotic GMA welding process', Robotics and Computer Integrated Manufacturing, vol. 19, pp. 567-572.

21. Ill-Soo Kima, Joon-Sik Sona, Sang-Heon Lee & Prasad KDV Yarlagaddac 2004, 'Optimal design of neural networks for control in robotic arc welding Robotics and Computer-Integrated Manufacturing, vol. 20, pp. 57-63.

22. Imran Bhamji, Michael Preussa, Philip L Threadgill, Richard J Moata, Adrian C Addisonc & Matthew J Peel 2010, 'Linear friction welding of AISI 304L stainless steel', Materials Science and Engineering vol. A 528 pp. 680-690.

23. Ion Mitele Victor Budau & Corneliu Craciunescu 2012, 'Dissimilar friction welding of induction surface-hardened steels and thermo chemically treated steels Journal of Materials Processing Technology, vol. 212, pp. 1892-1899.

24. Ivan J de Santana Balsamo Paulo & Paulo J Modenesi 2006, 'High frequency induction welding simulating on ferritic stainless steels', Journal of Materials Processing Technology, vol. 179, pp. 225-230.

25. Jinhong Zhu, Lin Li & Zhu Liu 2005 ' CO2 and diode laser welding of AZ31 magnesium alloy', Applied Surface Science vol. 247 pp.300–306.

26. Juang, SC & Tarng, YS 2002, 'Process parameter selection for optimizing the weld pool geometry in the tungsten inert gas welding of stainless steel', Journal of Materials Processing Technology, vol.122, pp. 33-37.

27. Khan, MMA, Romoli, L, Ishak, R, Fiaschi, M, Dini, G & De Sanctis, M 2012, 'Experimental investigation on seam geometry, microstructure evolution and micro hardness profile of laser welded martensitic stainless steels, Opt. Laser Technol. DOI:10.1016/j.optlastec.2011.11.035, vol. 44, pp. 1611-1619

28. Kima, TH, Yuma, SJ, Hu, J, Spicer, JP & Abell, JA 2011, 'Process robustness of single lap ultrasonic welding of thin, dissimilar materials', CIRP Annals - Manufacturing Technology vol.60 pp. 17–20.

29. Kirana, DV, Basub, B & Dea, A 2012, 'Influence of process variables on weld bead quality in two wire tandem submerged arc welding of HSLA steel,' Journal of Materials Processing Technology, vol. 212, pp.2041-2050.

30. Koen Faes, Alfred Dhooge & Patrick De Baets 2009, 'Parameter optimisation for automatic pipeline girth welding using a new friction welding method' Eric Van Der Donckt,Wim De Waele 'Materials and Design, vol. 30, pp.581-589.

31. Koilraj, M, Sundareswaran, V, Vijayan, S & Koteswara Rao, SR 2012, 'Friction stir welding of dissimilar aluminum alloys AA2219 to AA5083 Optimization of process parameters using Taguchi technique', Materials and Design, vol. 42. pp. 1-7.

32. Koleva, E 2005, 'Electron beam weld parameters and thermal efficiency improvement', Institute of Electronics, Bulgarian Academy of Sciences, vol.77, pp.413-421.

33. Kumar, A & Sundarrajan, S 2009, 'Optimization of pulsed TIG welding process parameters on mechanical properties of AA 5456 Aluminum alloy weldments', Materials and Design, vol.30 pp.1288–1297.

34. Lakshminarayanan, AK & Balasubramanian, V 2008, 'Process parameters optimization for friction stir welding of RDE-40 aluminium alloy using Taguchi technique,' Trans. Nonferrous Met. Soc. China, vol.18, pp.548-554.

35. Lung Kwang Pan, Che ChungWang, Ying Ching Hsiao & Kye Chyn Ho 2004, 'Optimization of Nd:YAG laser welding onto magnesium alloy via Taguchi analysis', Optics & Laser Technology, vol.37, pp.33-42.

36. Massimo lanzoni, Mirko salomoni & Bruno ricco 2010, 'Seam Welding Monitoring System Based on Real-Time Electrical Signal Analysis', Welding Journal, vol. 89, pp. 218-223.

37. Mohammad Mousavi Anzehaee & Mohammad Haeri 2011 'Estimation and control of droplet size and frequency in projected spray mode of a gas metal arc welding (GMAW) process', ISA Transactions, vol. 50, pp.409-418.

38. Mumin & Sahin H Erol Akata 2003, 'Joining with friction welding of plastically deformed steel', Journal of Materials Processing Technology vol.142, pp.239-246.

39. Mumin Sahin 2005, 'Joining with friction welding of high-speed steel and medium-carbon steel', Journal of Materials Processing Technology, vol. 168 pp. 202-210.

40. Mumin Sahin 2007, 'Evaluation of the joint-interface properties of austenitic-stainless steels (AISI 304) joined by friction welding', Materials and Design, vol. 28, pp. 2244-2250.

41. Mumin Sahin, 2009 'Characterization of properties in plastically deformed austenitic-stainless steels joined by friction welding', Materials and Design vol.30, pp. 135-144.

42. Mustafa Kemal Bilici 2012 'Application of Taguchi approach to optimize friction stir spot welding parameters of polypropylene', Materials and Design vol. 35, pp. 113-119.

43. Mustafa Kemal Bilici, Ahmet Irfan Yükler & Memduh Kurtulmus 2011, 'The optimization of welding parameters for friction stir spot welding of high density polyethylene sheets', Materials and Design, vol. 32, pp. 4074-4079.

44. Mustafa Kemal Bilici, AhmetIrfan Yükler & Memduh Kurtulmus 2011, 'The optimization of welding parameters for friction stir spot welding of high density polyethylene sheets', Mater. Design. DOI:10.1016/ j.matdes. 2011.03.014, vol. 32, pp. 4074-4079.

45. Na, S-J & Lee, H-J 1996, 'A study on parameter optimization in the circumferential welding of aluminium pipes using a semi-analytical finite-element method GTA', Journal of Materials Processing Technology vol. 57, pp. 95- 102

46. Nandan, R, DebRoy, T & Bhadeshia, H.K.D.H, 2008, 'Recent advances in friction-stir welding – Process, weldment structure and properties Progress in Materials Science vol. 53, pp.980-1023.

47. Padmanaban, G & Balasubramanian, V 2010, 'Optimization of laser beam welding process parameters to attain maximum tensile strength in AZ31B magnesium alloy', Optics & Laser Technology, vol. 42, pp. 1253-1260.

48. Palani, PK & Murugan, N 2006, 'Sensitivity Analysis for Process Parameters in Cladding of Stainless Steel by Flux Cored Arc Welding,' Journal of Manufacturing Processes, vol. 8, pp.2-4.

49. Panneerselvam, K, Aravindan, S & Noorul Haq, A 2012, 'Study on resistance welding of glass fiber reinforced thermoplastic composites', Materials and Design, vol. 41, pp. 453-459.

50. Paventhan, R, Lakshminarayanan, PR & Balasubramanian, V 2011, 'Prediction and optimization of friction welding parameters for joining aluminium alloy and stainless steel,' Trans. Nonferrous Met. Soc. China, vol. 21, pp. 1480-1485.

51. Paventhan, R, Lakshminarayanan, PR & Balasubramanian, V 2012, 'Optimization of Friction Welding Process Parameters for Joining Carbon Steel and Stainless Steel', Journal of Iron and Steel Research, International.vol. 19, pp. 66-71.

52. Peter M Norman, Alexander FH Kaplan & Jan Karlsson 2010, 'Classification and generalization of data from a fibre-laser hybrid welding case,' Physics Procedia, vol. 5, pp.69–76.

53. Piekarska, W & Kubiak, M 2012, 'Modeling of thermal phenomena in single laser beam and laser-arc hybrid welding processes using projection method', Applied Mathematical Modelling, vol. 73, pp.43-48.

54. Piotr Lacki & Konrad Adamus 2011, 'Numerical simulation of the electron beam welding process', Computers and Structures, vol. 89, pp.977-985.

55. Ranfeng Qiu, Chihiro Iwamoto & Shinobu Satonaka 2009, 'Interfacial microstructure and strength of steel/aluminum alloy joints welded by resistance spot welding with cover plate', J. Mater. Proc. Tech. DOI:10.1016/j.jmatprotec.2008.11.003, vol. 209, pp. 4186-4193

56. Reisgen, U, Schleser, M, Mokrov, O & Ahmed, E 2012, 'Optimization of laser welding of DP/TRIP steel sheets using statistical approach', Optics & Laser Technology, vol. 44, pp. 255-262.

57. Reisgen, U, Schleser, M, Mokrov, O & Ahmed, E 2012, 'Optimization of laser welding of DP/TRIP steel sheets using statistical approach', Opt. Laser Technol, DOI:10.1016/j.optlastec.2011.06.028, vol. 44, pp. 255-262

58. Ruckert, G, Huneau, B & Marya, S 2007, 'Optimizing the design of silica coating for productivity gains during the TIG welding of 304L stainless steel', Materials and Design, vol. 28 pp. 2387-2393.

59. Saeid Hoseinpour Dashatan,Taher Azdast, Samrand Rash Ahmadi & Arvin Bagheri 2013, 'Friction stir spot welding of dissimilar polymethyl methacrylate and acrylonitrile butadiene styrene sheets,' Materials and Design, vol. 45, pp.135-141.

60. Sathiya, P, Abdul Jaleel, MY, Katherasan, D & Shanmugarajan, B 2011, 'Optimization of laser butt welding parameters with multiple performance characteristics', Opt. Laser Technol. DOI:10.1016/j.optlastec.2010.09.007, vol. 43, pp. 660-673

61. Sathiya, P, Panneerselvam, K & Soundararajan, R 2012, 'Optimal design for laser beam butt welding process parameter using artificial neural networks and genetic algorithm for super austenitic stainless steel', Optics & Laser Technology, vol. 44, pp.1905-1914.

62. Sathiya, P, Abdul Jaleel, MY, Katherasan, D & Shanmugarajan, B 2011, 'Optimization of laser butt welding parameters with multiple performance characteristics', Optics & Laser Technology, vol. 43, pp.660-673.

63. Sathiya, P, Aravindan, S, Noorul Haq, A & Paneerselvam, K 2009, 'Optimization of friction welding parameters using evolutionary computational techniques', journal of materials processing technology, vol. 209, pp. 2576-258.

64. Satyanarayana, VV, Madhusudhan Reddy, G & Mohandas, T 2005, 'Dissimilar metal friction welding of austenitic–ferritic stainless steels', Journal of Materials Processing Technology, vol.160, pp.128-137.

65. Tarng, YS, Juang, SC & Chang, CH 2002, 'The use of grey-based Taguchi methods to determine submerged arc welding process parameters in hardfacing', Journal of Materials Processing Technology, vol.128, pp.1-6.

66. Tarng, YS, Tsai, HL & Yeh, SS 1999, ‘Modeling, optimization and classification of weld quality in tungsten inert gas welding’, International Journal of Machine Tools & Manufacture, vol.39, pp.1427-1438.

67. Timur Canel A, Ugur Kaya & Bekir Celik 2012, 'Parameter optimization of nanosecond laser for microdrilling on PVC by Taguchi method', Opt. Laser Technol. DOI:10.1016/j.optlastec.2012.04.023, vol. 44, pp. 2347-2353.

68. Tomasz Sadowski, Przemysław Golewski & Marcin Knes 2014, 'Experimental investigation and numerical modelling of spot welding–adhesive joints response', Compos. Struct. DOI:10.1016/j. compstruct. 2014.01.008, vol. 112, pp. 66-77.

69. Vidyut Dey, Dilip Kumar Pratihar, Datta, GL, Jha, MN, Saha,TK & Bapat, AV 2009, ‘Optimization of bead geometry in electron beam welding using a Genetic Algorithm journal of materials processing technology, vol. 209, pp. 1151-1157.

70. Vural, M 2014, 'Welding Processes and Technologies', Compre. Mater. Proc. DOI:10.1016/B978-0-08-096532-1.00601-4, vol. 6, pp. 3-48

71. Yang dongxia, Li xiaoyan, He dingyong, Nie zuoren & Huang hui 2012, ‘Optimization of weld bead geometry in laser welding with filler wire process using Taguchi’s approach’, Optics & Laser Technology vol. 44, pp. 2020–2025.

72. Yang dongxia, Li xiaoyan, He dingyong, Niezuoren & Huang hui 2012, 'Optimization of weld bead geometry in laser welding with filler wire process using Taguchi’s approach', Opt. Laser Technol. DOI:10.1016/j.optlastec. 2012.03.033, vol.44, pp. 2020-2025

73. Yangyang Zhao, Yansong Zhang Wei Hu & Xinmin Lai 2012, ‘Optimization of laser welding thin-gage galvanized steel via response surface methodology’, Optics and Lasers in Engineering, vol.50, pp.1267-1273.

74. Yong-Ak Songa & Sehyung Parka Soo-Won Chae 2005, ‘3D welding and milling: part II—optimization of the 3D welding process using an experimental design approach’, International Journal of Machine Tools & Manufacture 2005, vol. 45, pp.1063-1069.

75. Yousefieh, M, Shamanian, M & Saatchi, A 2011, ‘Optimization of the pulsed current gas tungsten arc welding (PCGTAW) parameters for corrosion resistance of super duplex stainless steel(UNS S32760) welds using the Taguchi method’, Journal of Alloys and Compounds vol. 509, pp. 782-788.